Alternate Atlantic forest and climate phases during the early Pleistocene 41 kyr cycles in southeastern Brazil

Paula A Rodríguez-Zorro, Marie-Pierre Ledru, Charly Favier, Edouard Bard, Denise C Bicudo, Marta Garcia Molina, Gisele Marquardt, Frauke Rostek, André O Sawakuchi, Quentin Simon, et al.

Paula A. Rodríguez-Zorro, Marie-Pierre Ledru, Charly Favier, Edouard Bard, Denise C. Bicudo, Marta Garcia, Gisele Marquardt, Frauke Rostek, André O. Sawakuchi, Quentin Simon, Kazuyo, Alternate Atlantic forest and climate phases during the early Pleistocene 41 kyr cycles in 3 Southeastern Brazil Quaternary Science Reviews, 2022, 286, 107560
DOI : 10.1016/j.quascirev.2022.107560

Alternate Atlantic forest and climate phases during the early Pleistocene 41 kyr cycles in 3 Southeastern Brazil

Paula A. Rodríguez-Zorro[1*], Marie-Pierre Ledru[1], Charly Favier[1], Edouard Bard[2], Denise C. Bicudo[3], Marta Garcia[2], Gisele Marquardt[4], Frauke Rostek[2], André O. Sawakuchi[5], Quentin Simon[2], Kazuyo Tachikawa[2]

1. ISEM, Univ Montpellier, CNRS, EPHE, IRD, 34095, Montpellier, France.
2. CEREGE, Aix Marseille Univ, CNRS, IRD, INRAE, Coll France, 13545, Aix-en9 Provence, France.
3. Environmental Research Institute, Department of Biodiversity Conservation, Av. Miguel Estéfano 3687, 04301-012 São Paulo, SP, Brazil
4. University of Guarulhos, Centro de Pós-Graduação, Pesquisa e Extensão CEPPE, Praça Tereza Cristina 88, 07023-070 Guarulhos, SP, Brazil
5. Institute of Geosciences, University of São Paulo, São Paulo, Brazil

*First author current affiliation: Escuela de Biociencias, Facultad de Ciencias, Universidad 1Nacional de Colombia-Sede Medellín, Colombia. email: paularsat@gmail.com

Keywords: Subtropical front, Araucaria, southern hemisphere, Antarctic ice volume, Tropical forest

Abstract: The early Pleistocene was driven by 41 kyr glacial cycles that have been rarely characterized in continental records, especially in South America. Most of long-term records derive from marine records (*e.g.* sea surface temperatures (SST)) and have been widely used to infer past climate dynamics but implications for the continent have rarely been evaluated. We present an early Pleistocene record (COL17c) from the Colônia basin in the Atlantic forest domain in southeastern Brazil. Our aim was to integrate past environmental dynamics and the drivers of change between ca. 1.5 to 1.3 Myr at the latitude of Colônia (23°S; ca. 700 m a.s.l.). We applied a multi-proxy approach including pollen, charcoal, X-Ray fluorescence scanning (XRF), biomarkers and diatoms. We identified three glacial periods and four interglacials containing a continuous cool forest, mainly dominated by *Araucaria*. The glacial periods were characterized by increases in organic matter input on the lake, semi-deciduous forest, and shore and herbaceous vegetation. In contrast, the interglacials were marked by increases in evergreen forest and reduced organic matter input. We attribute these alternating phases of vegetation and lake productivity to meridional temperature differences that regulated the input of moisture at the latitude of Colônia. After 1.430 Myr, glacial and interglacial periods showed a different dynamism with an increase in cool forests and drops in relative temperature, concomitant with regional long-trend cooling observed in marine records. The observed forest responses inferred from the COL17c record are in phase with regional climate features such as the development of the cold Pacific tongue and the equatorward migration of subpolar fronts, highlighting the strong influence of the Southern Hemisphere at Colônia during the early Pleistocene.

Introduction

A major challenge to testing the responses of tropical diversity to climate change is the scarcity of continuous long sediment records associated with the succession of glacial and interglacial cycles. The Pleistocene was characterized by two types of glacial-interglacial cycles, 41 kyr and 100 kyr cycles, with an intermediary phase, the mid-Pleistocene transition (MPT), between 1.25 and 0.7 Myr (Clark et al., 2006; Schackleton and Opdyke, 1976). The Pleistocene started 2.58 Myr ago (Head et al., 2021) with the

onset of Northern Hemisphere glaciations and the beginning of cooling of the subtropical zones, expressed differently depending on latitude (Ravelo et al., 2004). In the Southern Hemisphere, the early Pleistocene was marked by increased contributions of subtropical surface waters to the Sub-Antarctic Atlantic (*i.e.* ODP site 1090; Martinez-Garcia et al., 2010) caused by the equatorward expansion of the polar and subpolar frontal systems and the associated contraction of the subtropical gyres between 1.8 and 1.2 Myr (Fig. 1) (Becquey and Gersonde, 2002; Martinez-Garcia et al., 2010; McClymont et al., 2013). A rapid increase in Antarctic ice volume was observed at 900 kyr while the persistence of freezing temperature has been observed in the southern ocean at every glacial maximum at least since 1.5 Myr (Elderfield et al., 2012; McClymont et al., 2013 and literature therein). Today, the subtropical front (STF) is located in the western portion of the Atlantic sector at 40°S (Graham and De Boer, 2013).The location of the STF has varied over time and migrated proportionally to the severity of each glacial period (Bard and Rickaby, 2009) in phase with the Antarctic expansion of glacial sea ice (Hou et al., 2020; McClymont et al., 2013) and the northward shift of the polar front isotherms (Becquey and Gersonde, 2002).

Few sedimentary archives are available to assess the impact of these strong oceanic and atmospheric reorganizations on vegetation during the early Pleistocene. In the Northern Hemisphere, Mediterranean vegetation assemblages show profound changes from the Pliocene to the present with the decline of subtropical taxa and the establishment of xeric vegetation (Combourieu-Nebout et al., 2015). In the tropics, the closest relatives of many extinct or highly restricted taxa such as the conifer *Araucaria* are generally found today in cooler tropical mountain tropical areas (Ledru and Stevenson, 2012). In southeastern Australia, between 1.84 and 1.56 Myr, climate reconstruction based on beetles and pollen deposited in a paleolake (37°S), showed a temperature that was warmer than today and high humidity year round (Sniderman et al., 2007, 2009). These conditions imply large scale changes in circulation compared to current winter-dominant rainfall regimes. Near the equator in South America, the composite Funza09 pollen record (4°N, 2550 m a.s.l.) located in the Bogotá basin (Colombia) covers the last 2.24 Myr. The basin was composed of wetlands and swamps until ca.1.3 Myr when faster subsidence of the basin floor transformed the zone into a big deep lake that lasted until the MPT (Torres et al., 2013). Upward shifts in the tree line in the region were paced by the succession of the glacial interglacial cycles (Torres et al., 2013). Despite the existence of such record, there is no clear description of the environmental dynamics and the climatic system that dominated during the early Pleistocene in South America. Here we present the palaeoenvironmental characterization of an early Pleistocene section from the COL17c composite record (1.5 Myr; Simon et al., 2020) for the Colônia basin. We integrate past vegetation dynamics and drivers of change in an unexplored period in the South American tropics in the Atlantic forest domain in southeastern Brazil. Today, the Brazilian Atlantic forest domain occupies a 3,500 km latitudinal range extending from the Equator to southern Brazil (Fig. 1). In southeastern Brazil, the domain is composed of a narrow coastal evergreen rainforest, a semi-deciduous forest in the hinterland that occupies the largest area, and a subtropical forest characterized by the ancient conifer *Araucaria,* covering the extensive inner highlands (Oliveira-Filho and Fontes, 2000). At higher altitudes with shallower soils, the Atlantic forest merges with high elevation grasslands (Scheer and Mocochinski, 2009). The different forest expressions are related to rainfall distribution in the winter and summer regimes, and temperatures in winter or the occurrence of frost (Fig. 1; Oliveira-Filho et al., 2015). In austral winter, the climate in this region is mainly influenced by northward shifts of polar air masses (e.g. the STF) resulting in permanent drizzle and moisture. In contrast, during austral summer, the climate is strongly influenced by the South American summer monsoon (SASM) and the position of the South Atlantic Convergence Zone (SACZ) (see Fig. 1 in Rodríguez-Zorro et al., 2020). Following the penultimate glacial period the Brazilian Atlantic forest responded to climate changes regulated by the SASM and the polar air masses (Rodríguez-Zorro et al., 2020). First, a northern shift of the STF during the penultimate glacial allowed the northward expansion of the *Araucaria* forest in the region (Rodríguez-Zorro et al., 2020). Then, starting at 95 kyr, climate reorganizations related to dominance of the SASM over the influence of the polar masses regulated forest expansion and regression phases that were mainly driven at precession scale (Cruz et al., 2005; Rodríguez-Zorro et al., 2020). High altitude grasslands in southern Brazil show that they were covered with grassland until the expansion of the

subtropical forest in the last 3,000 years under a year-round rainfall regime (*e.g.* Behling, 2000; Jeske-Pieruschka et al., 2013, Ledru et al., 2016). In fact, phylogeography showed that forest fragmentation explains the species divergence observed during the late Pliocene and early Pleistocene, likely paced by climatic oscillations (Batalha-Filho et al., 2019). In the existing studies from the Atlantic forest domain three phylogenetic groups have been identified according to their geographical location: south, central and north. Differences have been attributed either to geographical barriers or to different patterns of climate change (e.g., Batalha-Filho and Miyaki, 2016; Carnaval et al., 2009). If according to D'Horta et al. (2011), the northern and south-central groups are separated and antiphased, other analyses suggest specific evolutionary patterns indicating spatial variation between the southern and central groups in the persistence of these forests during the Pleistocene (e.g., de Sousa et al.,2020; Thomé et al., 2010). In light of the changes in glacial-interglacial cycles, ice volume and temperature throughout the Pleistocene, we would infer marked modifications in the distribution and floristic composition of the tropical Atlantic forest to explain both past fragmentation and the modern patterns.

The aim of the present study was to characterize early states of the Atlantic forest to evaluate the link with southern hemisphere climate variability at orbital scales using a sediment core located at the transition between SASM and subtropical front influences, which is also located between the central and southern phylogeographic groups. The COL17c composite record was analyzed based on pollen, charcoal, elemental composition of bulk sediment obtained by X-Ray fluorescence scanning (XRF), biomarkers (branched glycerol dialkyl glycerol tetraethers (brGDGTs), n-Alkanes and Hopanes) and diatom material.

Study area

The COL17c composite record was taken from the Colônia basin (23°52′03″S, 46°42′27″W, ca. 700 m a.s.l.), São Paulo, Brazil. Colônia is a crater-like structure with an annular ring of hills reaching 925 m a.s.l. and an inner depression characterized by a wetland and alluvial plain mainly filled with alluvial sediments (Prado et al., 2019; Riccomini et al., 2011). The regional climate is strongly influenced by northward shifts of polar air masses that result in permanent drizzle and moisture in winter (JJA), while during austral summer (DJF), the regional climate is affected by the SASM and the position of the SACZ (see Fig. 1 in Rodríguez-Zorro et al., 2020). Mean annual precipitation is 1,600 mm, including two months with less rainfall in austral winter (a short dry season in July and August), but natural fires nevertheless do not occur during this period due to high moisture availability in the area.

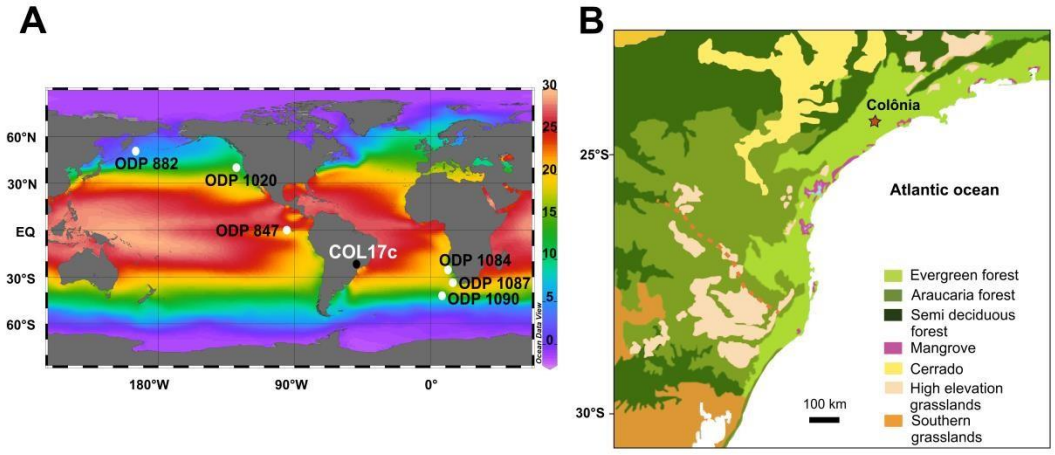

Figure 1. Study site. A) Location of Colônia and marine sea surface temperature (SST-°C) records reporting a cooling during the early Pleistocene (1.8 to 1.2 Ma) according to McClymont et al. (2013). B) Vegetation types in southeastern Brazil between ca. 20 and 30 °S. The red star shows the location of Colônia. The map in A) was generated with Ocean Data View software, (Schlitzer, 2021) using the modern annual mean SST values from the World Ocean Atlas 2018 (WOA18; Boyer et al., 2018). For more details on the basin see Riccomini et al., 2011; Prado et al., 2019 and Simon et al., 2020.

The mean annual temperature is 20 °C and the average winter temperature is ~17 °C (Rodríguez-Zorro et al., 2020).
The rim surrounding the Colônia basin is covered by Atlantic rainforest mainly represented by the families Myrtaceae, Rubiaceae, Bromeliaceae,Arecaceae, along with other evergreen forest species (Garcia and Pirani, 2005). The swamp located in the center of the basin is dominated by Poaceae, Xyridaceae (*Xyris*), Lentibulariaceae, Sphagnaceae (*Sphagnum*) and Asteraceae. Forest patches inside the basin are represented by Myrtaceae, Melastomataceae, Arecaceae and Cyatheaceae (Garcia and Pirani, 2005, Camejo et al., 2022).

Methods

Coring and sampling

The COL17c record is composed of 5 parallel core sections reaching a total of 52 m corrected depth (COL17-1(14.7 m), COL17-2(51 m), COL17-3(52 m), COL18 (2 m) and COL19 (8 m) (Simon et al., 2020). In the present study, we analyzed the deepest part of the record corresponding to a lacustrine section from cores COL172 and COL17-3, between 45.99 to 51.71 meters composite depth (mcd), with 93% sediment recovery. The COL17-2 and COL17-3 cores were drilled using a built-in pushing corer with rotary tubing mounted on a 6T Caterpillar® drill rig (Simon et al., 2020). Following sedimentological description, the core sections (1.5 m long) were sampled with u-channels (rigid u-shaped plastic liners, 2x2 cm cross section) from the center of the working halves for magnetic and XRF analyses (Simon et al., 2020). Each cm of the working halves was then sampled for biological proxies (pollen, diatoms and biomarkers). Samples were stored in zip-lock bags at 4 °C in a dark room at ISEM, University of Montpellier, France.

XRF analyses

High-resolution non-destructive elemental analysis was performed using an XRF core scanner (ITRAX, Cox Analytical Systems) at CEREGE. The relative abundance of Si, K, Ti and Rb was measured to estimate the variability of detrital inputs, while the ratio of Compton scatter (incoherent) to Rayleigh scatter (coherent), inc/coh ratio, was used to represent variations in the relative proportions of light and heavy elements, a proxy for organic matter content (Croudace et al., 2006). The measurements were made at 5mm spatial resolution at 30 kV and 45mA with 15 s of counting with a Mo tube as the X-ray source.

Biomarkers: brGDGTs, n-Alkanes and Hopanes

For the analysis of branched glycerol dialkyl glycerol tetraethers (brGDGTs), nalkanes and hopanes, 0.3 to 0.4 grams of freeze-dried and mortar-ground sediment from 51 samples were extracted using an accelerated solvent extraction system (ASE350, Thermo Scientific). The lipid extracts were first separated into non-polar (containing n-alkanes and hopanes) and polar fractions (containing brGDGTs) by Alumina B gel column chromatography (Supelco) followed by an additional cleanup of the non-polar fraction on a Si-Ag column. brGDGTs were analyzed by HPLC-MS following the method described by Hopmans et al. (2016) and adapted at CEREGE by Davtian et al. (2018), and described in detail for the record CO14 in Rodríguez-Zorro et al. (2020). n-alkanes and hopanes were analyzed using a FID equipped gas chromatograph (Thermo Scientific Trace GC), a 60 m x 0.25 mm x 0.1 μm non-polar fused silica column DB-5-MS (J&W) fitted with a 2.5 m x 0.53 μm deactivated retention gap and using hydrogen as carrier gas. Concentrations of n-alkane and hopane were determined by comparison with an internal standard (hexatriacontane).
In order to estimate the origin of brGDGTs and to select the most appropriate calibration for the reconstruction of the mean annual air temperature (MAAT), we used the ratio of specific brGDGTs as qualitative indicators of terrestrial organic matter versus aquatic production: the brGDGTS ∑IIIa/∑IIa

and the branched and isoprenoid tetraether (BIT) index (See Methods section in Rodríguez-Zorro et al. (2020) and literature therein). We calculated temperature anomalies with respect to the mean over the full record by using several soil- and peat-specific temperature calibrations (de Jonge et al., 2014; Martínez-Sosa et al., 2021; Naafs et al., 2017a, 2017b; Véquaud et al., 2022) as well as two lake temperature calibrations (Martínez-Sosa et al., 2021; Russell et al., 2018; Fig. 3a).
The concentration of long-chain n-alkanes, expressed as the sum of C24 to C35alkanes concentrations, is a well-known contribution of terrestrial plants to the organic matter in soils and lake sediments. Hopanes and brGDGTs are also abundant in lake sediments and peat, corresponding to the bacterial contribution to the sediment (Innes et al., 1997; Weijers et al., 2006). Hopanes and brGDGTs can originate from bacterial production in the lake or be transported into the sediments among terrestrial organic matter.

Pollen and charcoal analyses

A total of 138 pollen samples were taken from the undisturbed sections of the COL17c. The sampling resolution was of 4 cm based on the liner depth of each of the core sections. The depth of the samples was corrected to mcd based on (Simon et al., 2020).
The pollen samples were prepared using 0.5 cm^3 sample volume, and treated with 40% HF, 15% HCl and 10% KOH. For better pollen preservation, we omitted sieving and acetolysis. *Lycopodium clavatum* tablets were added to calculate pollen, spore and microcharcoal concentrations (Stockmarr, 1971). We took care to add a minimum of 30,000 *L.clavatum* spores per sample as we used different batches of tablets (#3862, #1031, and #161018201; with a mean spore number per batch of 9,666, 20,848, 17,461 respectively).
Pollen counting was based on at least 400 terrestrial pollen grains per sample, excluding aquatic taxa and spores. Pollen and spore identification was based on pollen reference literature (Lorente et al., 2017; Lorscheitter et al., 1999, 1998), the Atlantic forest reference collection belonging to the department of Geosciences at the University of Campinas, Brazil, and the pollen reference collection belonging to ISEM, University of Montpellier, France. Pollen ecological grouping of the terrestrial pollen sum was based on the local vegetation survey conducted by Garcia and Pirani, (2005), literature on regional southeastern Brazil (Colli-Silva et al., 2021; Garcia et al., 2004; Marchant et al., 2002; Montade et al., 2019; Neves et al., 2017; Pennington et al., 2000) and the Brazilian flora checklist (Flora do Brasil, 2020). Terrestrial pollen taxa were grouped as evergreen forest (EF), semideciduous forest (SDF), cool taxa indicators (AF-*Araucaria* dominated cool forests) and herbaceous vegetation (see Supplementary Material Fig.1).
The number of zones in the pollen diagram was based on terrestrial pollen sum using optimal splitting by sums-of squares. The number of statistically significant zones was then evaluated using the broken stick model (Bennett, 1996). The pollen diagram was drawn and zones were analyzed using Psimpoll (Bennett, 2009). Pollen sample richness was calculated using rarefaction to a base of 400 counts (E (T400)) (Matthias et al., 2015; Rodríguez-Zorro et al., 2017). The non-metrical multidimensional scaling (NMDS) of the terrestrial pollen was applied using the package Vegan (Oksanen et al., 2015). The NMDS analysis included pollen taxa with a sum > 5% along the record. Microcharcoal particles were counted on the pollen slides without differentiation and expressed as concentration (particles/cm^3) based on (Finsinger and Tinner, 2005).
A total of 124 subsamples of 1 cm^3 were prepared for macro-charcoal analysis by treating them with bleach and KOH to concentrate the charcoal particles. The subsamples were then sieved through 160 μm mesh and analyzed under the microscope to separate the charcoal particles. The particles were counted and their size and area measured using WinSeedle software. The data used for this paper are expressed as the concentration of charcoal particles/cm^3.
Pollen data used for multi proxy comparison were analyzed using R Development Core Team, (2020).

Diatoms

A total of 87 samples from the section COL17-3 were analyzed, using the same resolution as for pollen. The sediment samples (0.5 cm^3 per sample) were cleaned using 30% H_2O_2 followed by 10% HCl, then heated at 90 °C for 1-6 hours to remove organic matter (Battarbee et al., 2001). Next, the samples were rinsed several times with deionized water to remove all supernatant fluids after digestion. The cleaned frustules were mounted in Naphrax (RI= 1.74). Relative abundance was estimated by counting at least 400 valves with an efficiency count of at least 90% (Pappas and Stoermer, 1996). Diatoms were identified by comparison with reference collections (e.g. Kulikovskiy et al., 2015; Metzeltin and Lange-Bertalot, 2007, 1998; Rumrich et al., 2000). Diatom analyses of the section COL17-2 are ongoing.

A total of 64 types of diatoms were found in COL17-3 and ecological grouping was based on the 8 dominant taxa. The first group contains the shallow water indicators including *Pseudostaurosira craterii, Planothidium scrobiculatum, Gomphonema* spp. *Eunotia* spp., an araphid diatom from the genus *Staurosirella* spp and an unidentified diatom *genus1.* Turbid environment indicators include *Aulacoseira granulata* and *A. ambigua* (Bicudo et al., 2016; Costa et al., 2017; Kociolek et al., 2015; Taylor et al., 2007).

Refining the age model

Applying the ^{10}Be age model (Simon et al., 2020) to the analyzed proxies, we observed analogous changes in the COL17c proxies, which displayed cycles close to the 41 kyr period. To refine the original ^{10}Be-based age model (Simon et al., 2020), we adjusted the sedimentation rate by fitting the depth cycles of XRF inc/coh ratio signal to a 41-kyr period (for further details and discussion see section 6.3 and Supplementary Material Figs. 2-4). We performed an evolutive harmonic analysis (EHA) using the Thomson multitaper method (Thomson, 1982) by applying the *eha* function of Astrochron R-package (Meyers, 2014) to linearly interpolate the inc/coh signal at 5mm resolution, with a 2.5 mcd window moved in 1 cm steps between frequencies of 0.2 cycle/m and 1.2 cycle/m. Then, at each depth in centimeter composite depth (cmcd) *z*, we determined the frequency *f(z),* expressed in cycles/m, with maximum F-test probability and computed the local sedimentation rate in cmcd/kyr as $s(z)=100(41.0 \cdot f(z))$. Next, the age model was anchored to maximize the correlation between the XRF inc/coh ratio and LR04 benthic δ^{18}O stack (Lisiecki and Raymo, 2005) and to fit a drop in reconstructed MAAT between 47.41 and 47.19 mcd to an observed drop in sea surface temperature (SST) from the record ODP-1090 (Martinez-Garcia et al., 2010) at around 1.434 Myr.

Results

Description of sediment and intensity of the XRF elements

The COL17c composite record is characterized by two distinct sedimentary units separated by a sharp transition: a) organic-rich silty-clayey brown-grey to greenish lacustrine sediments from 51.71 to 14.26 mcd, and b) organic rich peaty sediments from 14.26 mcd on (Simon et al., 2020). The cores analyzed in this study belong to the lacustrine unit from 51.71 to 45.99 mcd (ca. 6 meters in length). These lacustrine sediments are characterized by alternating bands of light brownish grey to black organic fine grained sediments. The sediments contain large quantities of mica grains, especially in sections with higher clay and silt contents. The disturbed sections in each sediment core are characterized by wet brown-yellowish siltyclayey mud intervals, easily recognizable by their typical "chimney" structure, parallel to the liner (Fig. 2 and Simon et al., 2020).

In the silty-clayey sections, the XRF intensities of Ti, K, Si, and Rb increased. Conversely, the dark organic layers showed high inc/coh ratios (i.e. the relative abundance of light and heavy elements; see Fig 3c, Simon et al., 2020 and Supplementary Material Figs.7 and 8).

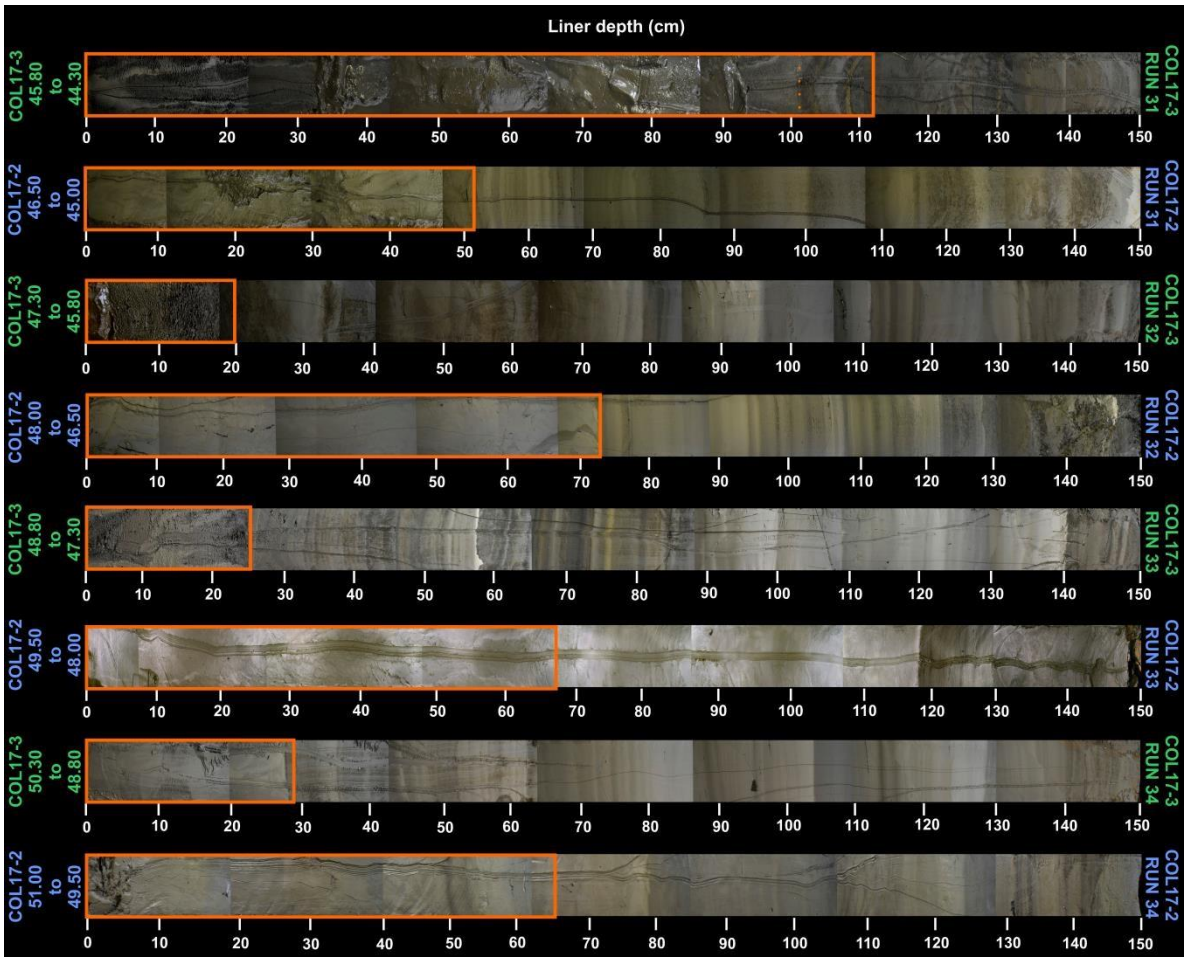

Figure 2. Sediment from the section 51.71 to 45.99 mcd, based on liner depth for COL17-2 and COL17-3 (see Simon et al., 2020). Orange rectangles identify the sections discarded from each liner (for more details see section 3 in Simon et al., 2020).

Biomarkers: MAAT anomalies based on brGDGTs, n-Alkanes, Hopanes and brGDGTs concentrations

The ∑IIIa/∑IIa ratio is on average ≈ 0.2 with a standard deviation of 0.03, and the BIT index is on average ≈ 0.9 with a standard deviation of 0.05. Both proxies suggest that the tetraethers are of terrestrial origin (Fig. 3b and see Methods section in Rodríguez-Zorro et al., 2020). The amplitudes of the MAAT curves are very different using the peat-soil (MAATs: 7 to 15°C) or lake calibrations (MAATs: 17 to 27°C). The highest MAAT values in COL17c using the peat calibrations (not shown) overlap with those obtained in the lacustrine section of CO14 (13 to 17°C using the peat calibration by Naafs et al. (2017b) and de Jonge et al. (2014); see Rodríguez-Zorro et al., 2020), however minima are cooler in COL17c. These temperatures are also lower than the seasonal range of modern temperatures in the region (15 to 25°C; INMET, 2020). Therefore, for interpreting the temperature data of core COL17c despite the lack of an adequate regional calibration, we have used temperature anomalies with respect to the mean MAAT of COL17c, obtained from the calibrations of Naafs et al. (2017a, 2017b), de Jonge et al. (2014), Russell et al. (2014), Martínez-Sosa et al., (2021) and Véquaud et al. (2022). The range of temperature anomalies (-5 to +4°C) is similar for the seven calibrations (Fig.3a). Another contribution of the tetraether analyses is their total concentration in the sediments (Fig. 3b). The sum of brGDGTs (IIa, IIa, Iabc) shows three prominent cycles synchronous with those observed in the in the pollen assemblages (Fig. 4) and the XRF inc/coh

ratio (Fig. 3c) which is a qualitative proxy for organic matter. These three organic matter cycles are also clearly expressed (Fig. 3b) in the total concentrations of C24-C35 n-alkanes, hopanes and the GDGT proxies (∑IIIa/∑IIa ratio, BIT).

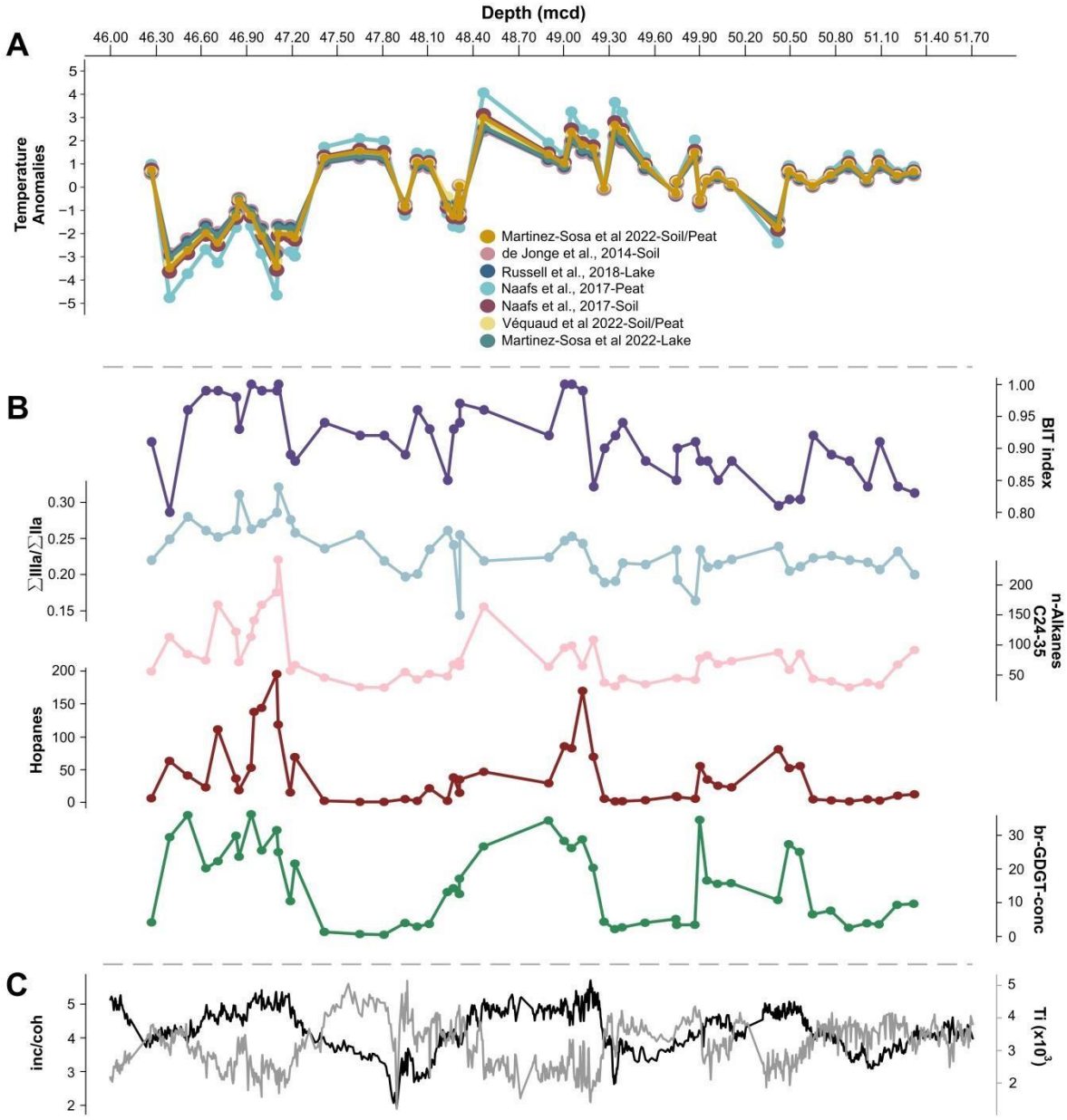

Figure 3. Biomarkers and selected XRF element intensities from the COL17c section 51.71 to 45.99 mcd. A) Mean annual air temperature (MAAT) anomalies with respect to the mean over the full record by using the Lake calibration (Russell et al., 2018: MAAT°C = 32.42xMBT′ 5ME − 1.21, RMSE ≈ ± 2.44), the soil and peat calibrations of Naafs et al.2017a, b (MAAT° Csoil=39.09xMBT′ 5ME - 14.50, RMSE≈ ± 4.1; MAAT° Cpeat = 52.18xMBT′ 5ME - 23.05, RMSE ≈ ± 4.7), soil calibration by de Jonge et al., 2014 (MAAT° C = 31.45xMBT′ 5ME - 8.57, RMSE ≈ ± 4.8), the lake and soil and peat calibrations of Martínez-Sosa et al., 2021 (MAAT° Clake=33.33MBT′ 5ME-0.075, RMSE≈ ±2.9; MAAT° Csoil&peat=38.46MBT′ 5ME-0.27, RMSE≈ ±3.9), and the soil and peat calibration of Véquaud et al., 2022 (MAAT° C=35.98xMBT′ 5ME-12.74, RMSE≈ ± 5.2) B) In purple, branched and isoprenoid tetraether (BIT) index, in light blue, ∑IIIa/∑IIa ratio of brGDGTs, in pink long-chain n-alkanes, in red Hopanes and in green the concentration of brGDGTs. C) XRF intensity of elements inc/coh and Ti.

Pollen, spores, charcoal and diatoms

Pollen was very well preserved throughout the sections analyzed, with relatively high concentrations (values between 44,845 and 38,3125 grains/cm^3). A total of 150 types of pollen and spores were identified (Fig. 4 and Supplementary Material Fig. 1).

In general, forest taxa dominated the analyzed interval, with mean frequencies of 80 ± 6 %, followed by 20 ± 6 % for herbaceous vegetation. The optimal splitting by sums-of squares of the terrestrial pollen sum and the broken stick model suggest

5 statistically significant zones with the lowest pollen sample richness in zones COL17c-1 and COL17c-4. The NMDS reached a convergent solution after 20 iterations (stress=0.16), using 83 taxa that met the criterion of having a sum >5% along the record (Fig. 5 and supplementary material Table 1). More negative NMDS1 values are attained by herbaceous vegetation and SDF taxa, while more positive values are attained by evergreen forest taxa. On the other hand, cool forest taxa had more negative NMDS 2 values, except for Ericaceae which seems to have more affinities with evergreen forest taxa (Figs. 4 and 5). Microcharcoal particles have a mean value of 18,490 ± 9,540 particles/cm^3, while macrocharcoal particles are rare, with values between 0 and 29 particles/cm^3.

Pollen zone COL17c-1 (51.71-50.65 mcd; 28 samples) is dominated by forest vegetation with high frequencies of evergreen forest (71 ± 5%), mainly characterized by *Podocarpus* (12-36%), *Ilex* (3-8%), Myrsine (10-25%) and Myrtaceae (4-14%). The SDF has on average 14 ± 4% including dominant taxa such as *Celtis* (0-4%), *Citharexylum* (0-4%) and Moraceae/Urticaceae (1-5%).

Lastly, cool forest (on average 2 ± 1%) is dominated by *Araucaria* (0-5%) and *Weinmannia* (0-2%). Herbaceous taxa are represented mainly with Poaceae frequencies (8 ± 2%). *Acaena* appears with values between 0 and 0.5 %. Pollen concentrations are relatively high with mean values of 135,417 ± 29,667 grains/cm^3. Shore vegetation is dominated by the macrophyte fern *Isoetes* with mean values of 17 ± 9%. Fern taxa represents the highest percentages of the record (mean of 18 ± 8%), with dominant elements such as tree ferns *Cyathea* (1-8%) and *Lophosoria* (1-10%), *Blechnum* (1-7%) and Polypodiaceae (1-9%).

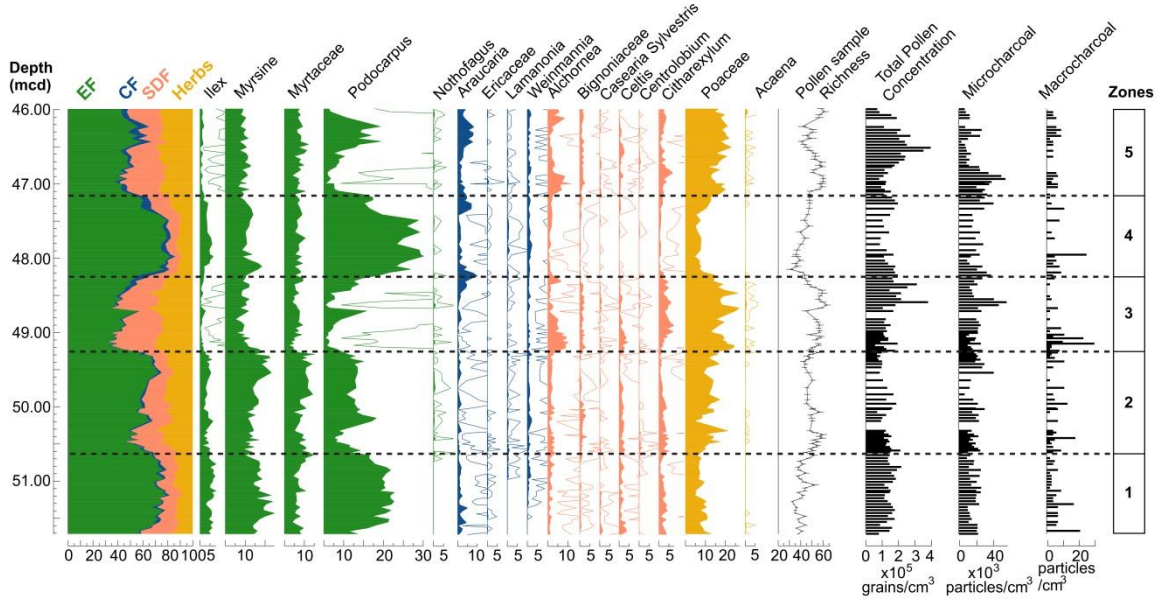

Figure 4. Pollen percentage diagram of 17 selected pollen taxa from the COL17c section 51.71 to 45.99 mcd. From left to right, Depth (mcd); Summary diagram of evergreen forest (EFgreen), Araucaria Forest (AF-blue), semi-deciduous forest (SDF-pink) and herbaceous (yellow) vegetation from Colônia. Pollen sample richness. Total pollen concentration (based on the pollen sum taxa) and micro/macrocharcoal concentration. Zones and dashed lines based on optimal splitting by sums-of squares. See full pollen diagram in Supplementary Material Fig. 1.

Aquatic taxa like the algae *Botryococcus* are the most frequent of the record (36 ± 14% on average). Diatoms indicating shallow environments show high values towards the top of the zone (from 50.81 to 50.65 mcd), some samples have zero diatom contents whereas others have high percentages, i.e. up to 98%. Diatoms indicating turbid environments are found in the same interval with the highest peak at a depth of 50.77mcd (54%). Concentrations of microcharcoal range between 7,340 and 2,4227 particles/cm^3 and concentrations of macrocharcoal between 0 and 20 particles/cm^3.

Pollen zone COL17c-2 (50.61-49.27mcd; 33 samples) is characterized by an increase in SDF (mean value of 18 ± 5%), including *Alchornea* (1-4%), *Celtis* (03%), *Citharexylum* (0-6%), Bignoniaceae (0-4%), Fabaceae (1-7%), among others. The frequencies of herbaceous taxa also increase (on average 20 ± 4%) dominated by Poaceae (4-21%), *Ambrosia* (0-5%), *Baccharis* (0-6%) and *Sauvagesia* (0-3%). *Acaena* oscilates between 0 and 0.4%. In contrast, evergreen forest taxa (mean value of 59±7%) such as *Ilex* (0-7%), Myrsine (2-15%), Myrtaceae (9-23%), and *Podocarpus* (5-26%) decrease. Cool forest have a mean value of 2 ± 1%. Pollen concentrations decrease with mean values of 110,288 ± 34,442 grains/cm^3. Tree fern taxa such as *Cyathea* (0-6%) and *Lophosoria* (0-5%) have low values in the bottom part of the zone but increase toward the top, while Polypodiaceae (1-5%) has higher frequencies at the bottom of the zone and decreases toward the top. The frequency of shore vegetation increases intermittently with mean values oscillating between 0 and 6%; *Juncus* appeares for the first time in the record in this phase (04%). The macrophyte *Isoetes* has the highest values of the entire record in the first part of the interval, however, its values decrease significantly toward the top of the zone (9-58%), whereas *Botryococcus* decreases slightly then remains stable with mean values of 28 ±11%. Diatoms indicating shallow environments have high values toward the bottom of the zone from 50.61 to 50.51 mcd and 50.34 to 50.02, with values ranging between 0 and 95%. Subsequently, diatoms in this group disappear from zone 2. Diatoms indicating turbid environments are only found at 50.56 and 50.02 mcd at low frequencies (1 and 10% respectively). Microcharcoal concentrations increase with mean values of 17,624 and 6,771 particles/cm^3. Macrocharcoal concentrations oscillate between 0 and 17 particles/cm^3. From this zone onward, frequencies of wind transported and non-native *Nothofagus aff. dombeyii* are found in the COL17c record (0-1%) (Fig. 4 and Supplementary Material Fig. 1).

Pollen zone COL17c-3 (49.24-48.27 mcd; 28 samples) is characterized by decreased forest vegetation, reaching the lowest values of the entire analyzed record (oscillating between 63 and 80%). Evergreen forest (41 ± 6%) taxa like *Ilex* (0-3%), *Myrsine* (5-18%), *Myrtaceae* (2-9%) and *Podocarpus* (1-22%) decrease in frequency, whereas the percentage SDF and herbaceous vegetation increase, oscillating between 13-

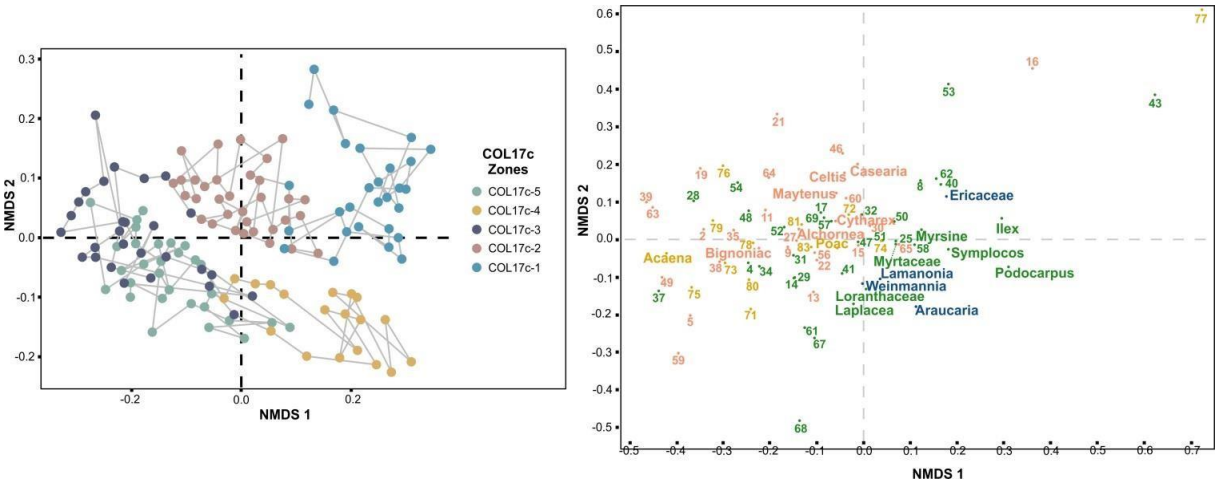

Figure 5. Non-metric multidimensional scaling analysis of pollen data from the COL17c section 51.71 to 45.99 mcd. On the left, samples plotted on depth differentiated by color based on the pollen data zones (optimal splitting by sums-of squares). On the right, the color of the pollen taxa refers to their associated forest type: green (EF), blue (cool tolerant taxa), pink (SDF) and yellow (Herbaceous). See Supplementary material Table 1 for taxa names.

40% and 20-37%, respectively. The SDF taxa whose frequency increase in this interval were *Alchornea* (0-10%), *Celtis* (0-5%), *Citharexylum* (1-8 %), Bignoniaceae (0-3%), Fabaceae (1-6%) and Moraceae/Urticaceae (3-11%). On the other hand, the frequency of cool forest vegetation (0-8%) is low at the bottom of the zone then increase toward the top, particularly the cool moisture sensitive *Araucaria* (0-6%). Herbaceous taxa represented by taxa such as *Acaena* (0-0.7%), *Baccharis* (1-5%), *Antidaphne* (05%), and Poaceae (13-27%) increase. The concentration of pollen is on average 148,222 ± 68,213 grains/cm^3. Polypodiaceae spores are more abundant than in zone 1 and 2 with values of 1 to 8%. Shore vegetation is mainly dominated by *Juncus,* which increases intermittently by 0 to 45%. *Botryococcus* oscillates between 8 and 45%. *Isoetes* values in this interval reach their lowest in the entire record (1-13%). Diatoms indicating shallow environments dominate the whole interval with mean frequencies of 77 ± 29%. Diatoms indicating turbid environments are only found at 49.02mcd at low frequencies (5%). Concentrations of microcharcoal are relatively high (mean value of 20,307 ± 10,695 particles/cm^3) and the highest values are found at 48.55, 48.59 and 48.63 mcd. In contrast, macrocharcoal is found at very low concentrations despite the fact the sample has the highest concentration of the record (at 49.14 mcd-29 particles/cm^3). *Pollen zone COL17c-4 (48.23-47.18 mcd; 19 samples)* is characterized by an increase in the frequencies of evergreen forest (on average 71 ± 9%) mainly dominated by *Podocarpus* (20-50%), *Ilex* (2-7%), and *Myrsine* (7-18%). Cool forest also increase (on average 5 ± 3%) with *Araucaria* (1-10%) and *Weinmannia* (1-2%) as the main contributors; the former being most abundant at the bottom and top of this period. SDF (mean value of 11 ± 4%) and herbaceous taxa (13 ± 3%) are reduced. Among the former, *Alchornea* (0-3%), *Celtis* (0-1%), *Citharexylum* (0-2%) are drastically reduced in frequency. Herbaceous

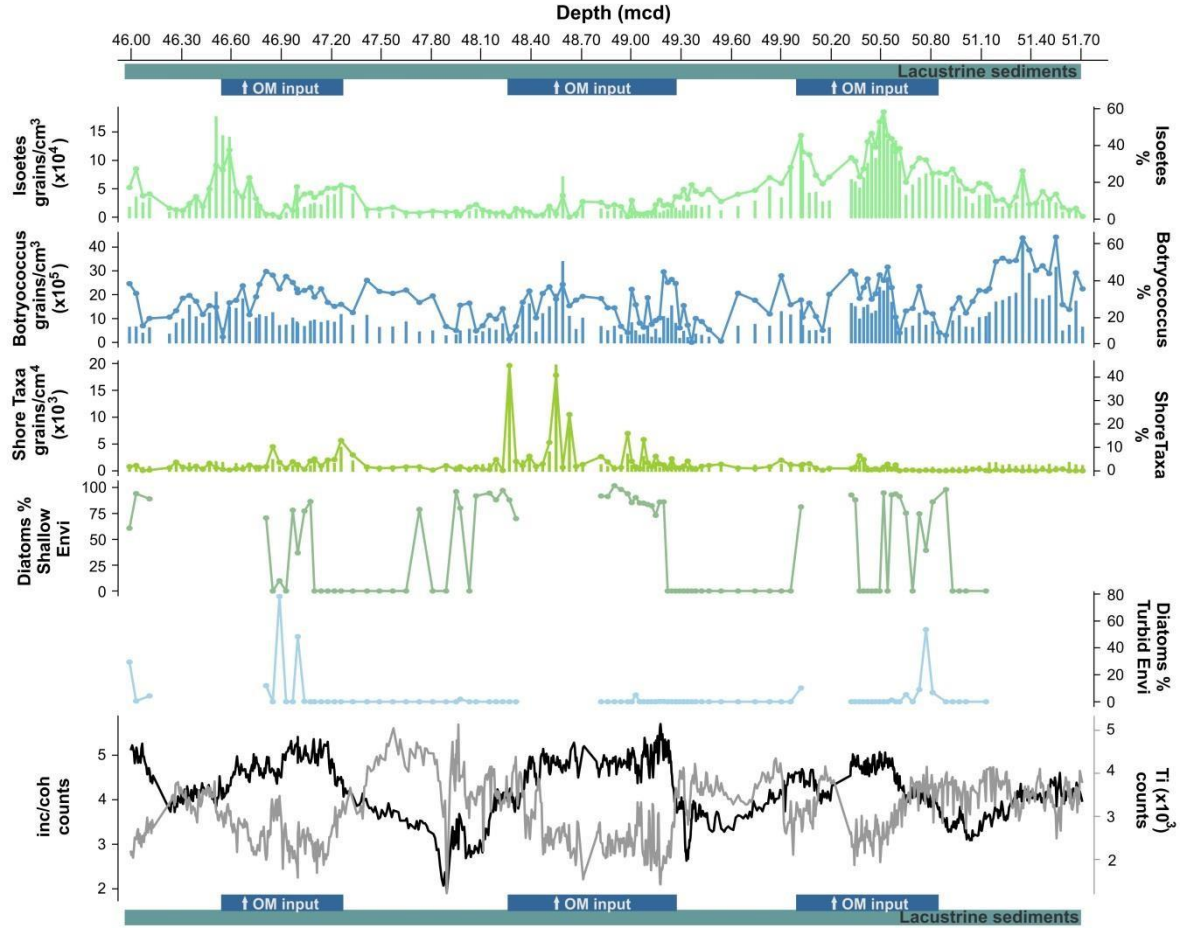

Figure 6. Local and lacustrine environment compared with the XRF element intensity of Ti and the inc/coh ratio in COL17c section 51.71 to 45.99 mcd. In the pollen data, the bars indicate concentrations and the dots and lines indicate percentages.

taxa such as Poaceae (415%), *Lobelia* (0-1%), *Acaena* (0-0.2%) and *Antidaphne* (0-1%) are strongly reduced compared to the previous interval. The pollen concentration is 133,904 ± 35,279 grains/cm^3. Tree fern taxa like *Cyathea* (1-5%) and *Lophosoria* (1-6%) again increase in frequency, whereas the frequency of Polypodiaceae decreases (13%). Shore taxa almost vanish during this period (0-12%), mainly dominated by Cyperaceae (0-2%) while *Juncus* (0-12%) reappears only in the upper part of the zone. Values of *Isoetes* (2-18%) are low in this interval, and only increase towards the top of the zone. *Botryoccocus* remains stable with mean values of 10 to 13%. Diatoms indicating shallow environments are found at the bottom of the zone with intermittent frequencies ranging between 0 and 97%. The concentration of microcharcoal is 21,517 ± 8,552 particles/cm^3, and that of macrocharcoal was 0 to 24 particles/cm^3.
Pollen zone COL17c-5 (47.14-45.99 mcd; 30 samples) is dominated by forest vegetation. The frequency of EF (46 ± 5%) decreases mainly with dominant taxa such as *Ilex* (0-2%) and *Podocarpus* (1-28%). The frequency of SDF forest increases its abundance with a mean of 25 ± 7% with dominant taxa such as *Alchornea* (1-12%), *Citharexylum* (0-7%), Bignoniaceae (0-3%), Fabaceae (1-5%), and Moraceae/Urticaceae (2-11%). Herbaceous taxa increase (mean value of 25± 3%) with dominant taxa such as Poaceae (11-23%), *Ambrosia* (0-4%), and *Baccharis* (1-5%). *Acaena* has the highest frequencies of the record oscillating between 0 and 1%. The concentration of pollen is the highest of the record with mean values of 162,137 ± 78,369 grains/cm^3. Shore vegetation increase slightly in the lower part of the interval mainly dominated by intermittent frequencies of *Juncus* (0-7%). *Isoetes* and *Botryococcus* also increase with mean frequencies of respectively 13 ± 8% and 31± 8%. Diatoms indicating turbid environments reappear in this interval with values oscillating between 0 and 74%. Diatoms indicating shallow environments dominate in the bottom and top sections of this interval with values oscillating between 0 and 94%. Concentrations of microcharcoal are high in the bottom part of the record with a maximum of 52,799 grains/cm^3, decreasing towards the top of the zone. Macrocharcoal particles are scarce (0-8 particles/cm^3).

Discussion

The laminated fine-grained sediments and diatom assemblages observed in the COL17c reflect the occurrence of a shallow lake in the basin of Colônia with alternating organic matter (OM) input phases (Figs. 2 and 6). Similarly, pollen data revealed seven phases of forest contraction and expansion, suggesting the influence of precipitation and temperature on the composition of regional vegetation. Such cyclicity with composite core depth allowed us to differentiate glacial and interglacial periods using indicative pollen taxa and assemblages (Fig. 4). Overall, a change in the cyclicity modalities occurred at 49.30 mcd, with changes of greater amplitude above this depth than below (Figs.5, 6 and 7). The existence of lacustrine diatoms (COL17-3 section), along with the continuous presence of *Botryococcus* indicates that Colônia remained a lake throughout the considered period. Three main phases of macrophyte and shore taxa expansion occurred during higher OM input at intervals around 50.85 and 50.02 mcd, 49.30 and 48.23 mcd and 47.30 and 46.50 mcd. Those phases were characterized by high frequencies of Isoetes as well as increases of grasses and shore taxa, such as Cyperaceae and Juncus (Fig. 6).Phases of OM input were inferred from peaks in the inc/coh ratio accompanied by C24-C35 n-alkanes, hopanes and the GDGT proxies (∑IIIa/∑IIa ratio, BIT), which further indicate that these lipids are mainly of terrestrial origin and transported into the lake (Fig. 3). Similarly, grasses and SDF that follow the same cyclicity indicate drier periods in the region (Fig. 7). Reduced OM input phases were observed in sediments with more silt and clay content, (with high relative abundance of terrigenous detrital indicators such as Ti, K, Rb, Si) with reduced nalkane and hopane concentrations and a lower inc/coh ratio. Wetter periods were inferred from EF and increased detrital inputs into the lake (e.g. high Ti counts).

Atlantic forest phases and inferred glacial-interglacial dynamics

The section of COL17c analyzed here showed that low temperatures played a key role in the expansion of Araucaria forests in the region (Figs. 5 and 6). At Colônia, Araucaria, a cold and moist sensitive taxon expanded simultaneously with the lowest Δ°T. Additionally, such trees grew along with other cold

sensitive taxa such as Weinmannia and Lamanonia, and evergreen forest taxa (Fig.5). Continuous cool conditions were inferred as well by the presence of the wind transported pollen of Nothofagus (although never observed in Brazil) that is currently observed in southernmost latitudes (e.g. Fontana and Bennett, 2012). On the other hand, two main species of Podocarpus grow in the region (Ledru et al., 2007). However, Podocarpus is a more complicated taxon to interpret since pollen morphology does not allow differentiation between species. P. sellowii, the only species observed today near Colônia (Garcia and Pirani, 2005), is tolerant to dry conditions, and grows at the transitions between gallery forests and Cerrados in central Brazil and high elevation forests and grasslands in southern and southeastern Brazil, while P. lambertii is tolerant to cold and frost conditions, and is restricted to Araucaria angustifolia forests (Ledru et al., 2007). The Podocarpus pollen found in the COL17c sequence might originate from the two different species. P. sellowii might have been present throughout the section and expanded during drier phases (e.g.pollen zone 3 or 5), while P. lambertii might have grown in the Araucaria forest when temperature decreased (Ledru et al., 2007).

Our record (COL17c) also highlights the significant role of water availability or the amount of precipitation in shaping vegetation dynamics in the Atlantic forest, at least during the studied

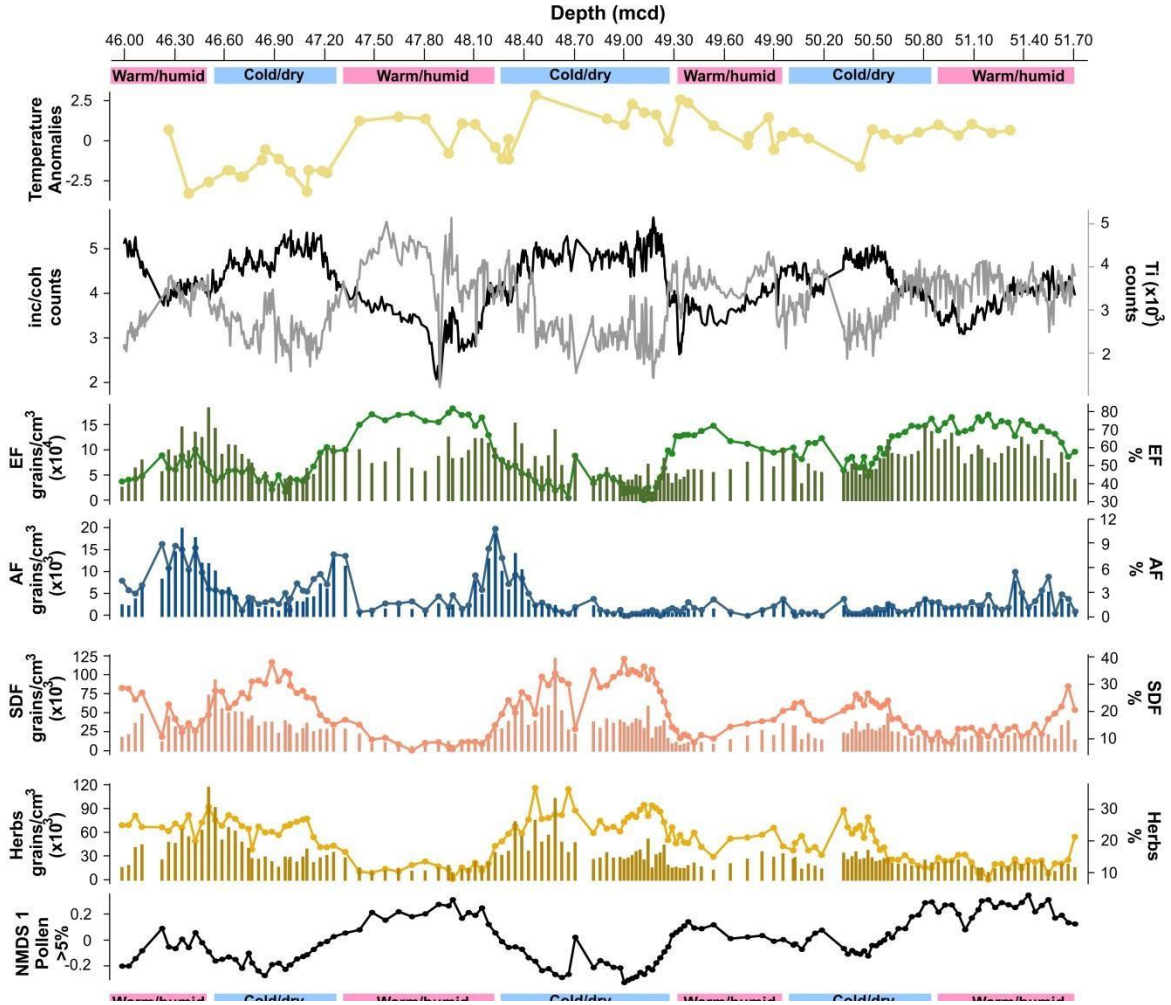

Figure 7. Vegetation responses in COL17c section 51.71 to 45.99 mcd. From top to bottom: MAAT anomalies based on the soil and peat calibration protocol by Véquaud et al. (2022); XRF element intensity from Ti and inc/coh ratio. Pollen concentrations and percentages from evergreen forest (EF-green), Araucaria (blue), semi-deciduous forest (SDF-pink) and herbaceous including grasslands (yellow); NMDS1 from the pollen taxa with a sum > 5% throughout the record. For pollen data, the bars indicate concentration values, and dots and lines indicate percentages per sample. Pink and blue bands highlight the seven discrete intervals with a characteristic environmental setting based on depth..

Quaternary section (Figs. 4,5 and 7). Nowadays, SDF is expanding inland and replacing rainforests as seasonal rainfall regimes include regular periods of drought (ca. 2-3 months) and where upslope adiabatic moisture is absent (Neves et al., 2017). Our pollen data suggest that precipitation amount may also have been a key factor in the expansion of such rich forests (Fig. 4 and Neves et al., 2017). At Colônia, the expansion of forests - with increases in semideciduous forest taxa - is associated with longer dry periods or reduced wet seasons than those that occur in the region today (Neves et al., 2017) (Figs.4, 5 and 7). This pattern was also observed in our record in parallel with the cyclicity of grasses and herbaceous vegetation, the inc/coh ratio and GDGT proxies (Figs. 6 and 7), between ca. 50.85 and 50.02 mcd, 49.30 and 48.23 mcd and 47.30 and 46.50 mcd, which point to drier regimes or regimes with less precipitation (see the grouping of vegetation with more negative values in the NMDS1 axis, Fig. 5). During those periods we observe also few pollen grains from Cerrado taxa such as Mauritia and Caryocar (see supplementary material for detailed description). Additionally, the presence of Acaena in our record, meant we could use it as indicator of dry periods (see it located with more negative values of NMDS1, Fig. 5), since this herb is currently not reported in vegetation surveys in the region of Colônia, and is only found further south in high elevation grasslands (Camejo et al.,2022; Kegler et al., 2010). The opposite effect, reflecting increase on moisture is seen with peaks on EF and the XRF detrital siliciclastic elements (Ti, K, Si and Rb) between ca. 51.71 and 50.85 mcd, 50.02 and 49.30 mcd, 48.23 and 47.30 mcd, and 46.50 and 45.99 mcd.

The analogous cyclicity of grasses, SDF and herbaceous vegetation with the inc/coh ratio, versus the synchronous cyclicity of EF with XRF detrital siliciclastic elements (Ti, K, Si and Rb) reflect differences between dry and wetter environments, respectively (Figs.4, 6 and 7). Although forest dominated the whole section, the grasses, herbaceous vegetation and SDF expanded three times when precipitation was reduced and periods of OM input occurred locally (Figs. 6 and 7). On the other hand, EF dominated during four intervals when moisture increased and high detrital inputs prevailed in the lake. Araucaria was observed throughout the record although it was more dominant after 48.40 mcd, i.e., synchronous with a decline in temperature observed in the Δ°T values (Figs. 3 and 7). Regional fires were observed throughout the section, although at lower magnitude than the fires observed in CO14 (Rodríguez-Zorro et al., 2020). Indeed, at COL17c the concentrations of charcoal were 10 times lower, suggesting that fires did not play an important role in shaping vegetation dynamics in our record (Fig. 4). In addition, the Δ°T showed no drastic changes in temperature like those observed in CO14. However, we observed a decreasing trend in temperature from 48.30 mcd towards the end of the record (see also *Araucaria* behavior in pollen zones COL17c-4 and 5).

Seven significant periods of change based on depth revealed alternating states of forest vegetation during the 51.71 to 45.99 mcd interval that we interpret as glacialinterglacial periods (Figs.5 and 7). The first interval (ca. 51.71 and 50.85 mcd) was characterized by the presence of a mixed evergreen forest with cool and moisture sensitive conifers Araucaria and Podocarpus, and evergreen trees such as Ilex and Myrtaceae. This configuration indicates humid and slightly cool conditions that can be characterized as an interglacial period. The effect of humid conditions can also be inferred from the presence of ferns that typically grow in cloud forests like Cyathea and Lophosoria, linked to the permanent presence of adiabatic moisture between ocean and high elevation (See Supplementary Material Fig. 1 and Rodríguez-Zorro et al., 2020). During the following interval (ca. 50.85 and 50.02 mcd), the increase in grasses, herbaceous and SDF taxa is evidence for a reduced precipitation regime under cool temperatures as AF dominated mainly by Araucaria. A dry period can be also inferred from the correspondence between the grasses, herbs, SDF, shore and macrophyte taxa expansion, and high inc/coh ratios. This interval was characterized as a glacial. The following interval (ca. 50.02 and 49.30 mcd), followed the opposite pattern, with increased EF, Ti abundance and a continuous AF, indicating moister and slightly warmer conditions (interglacial). A new phase was then detected with more marked changes (ca. 49.30 and 48.23 mcd) characterizing the interval with the largest expansion of grasses and herbaceous vegetation on the shore of the lake and increased SDF taxa, that we attributed to increased water deficit in the area. This effect was also reflected in the decrease in moisture sensitive tree taxa such Ilex and Podocarpus and the presence of dry environments indicator Acaena. In addition,

continuous AF support a cooler interval (glacial period) compared to the previous one. During the following interval (48.23 and 47.30 mcd), Ilex and Podocarpus underwent significant expansion. Araucaria forest was present during the entire interval with two peaks at the beginning and end, clearly following an increase in moisture, as indicated by an increase in EF taxa and drops in temperature as seen in the Δ°T curve (Figs. 3 and 7). This interval was characterized by slightly warmer and humid conditions (interglacial) similar to those observed during the interval between ca. 51.71 and 50.85 mcd (Figs.5, 6 and 7). The following interval (47.30 and 46.50 mcd) contained the biggest differences in Δ°T, increases in Araucaria as well as in grasses, Acaena, SDF and in the inc/coh ratio, indicating cool dry conditions (glacial). Lastly, between 46.50 and 45.99 mcd, inputs of moisture were evidenced by the biggest expansion of Araucaria (sensitive to increases on moisture, see Tagliari et al., 2021), increases in the abundance of Podocarpus, Ilex, Myrtaceae and Ti, indicating cool and moister conditions (interglacial). High frequencies of Araucaria during these last two intervals are in phase with the lowest Δ°T changes (47.10 and 46.39 mcd) and moisture increases at Colônia.

Based on composite depth we could infer that these variations in forest composition and OM input were related to the dynamics of meridional temperature differences as also inferred during the penultimate glacial in the region (CO14; see current climatic setting at Colônia in Fig. 1 in Rodríguez-Zorro et al., 2020). During glacial periods in this early Pleistocene section (COL17c), northern incursions of polar fronts and an ITCZ placed further north (Seo et al., 2015), enabled the expansion of grasslands and SDF taxa, clearly reflecting a diminished SASM system (reduction in moisture from the tropics). Conversely, during interglacial periods, a reduced effect from the south, although still present in the area (low temperatures and continuous AF), enabled the expansion of EF taxa. During these periods, it seems that increased humidity greatly favored taxa such as *Podocarpus* as well as cool moisture tolerant *Araucaria*, which expanded most during glacial-interglacial transitions (inception and termination), as also observed in CO14 (Rodríguez-Zorro et al., 2020). The fact that *Araucaria* was highly abundant during glacial-interglacial transitions, as also observed in CO14, reflects the restricted moisture input during glacial periods. Moreover, in our early Pleistocene record, the effect of the SASM and therefore precession paced precipitation (Cruz et al., 2005) seems to be minimal due to the strong influence of the southern ocean atmospheric circulation. This is the opposite of what we observed during the last 95 kyr in the region (CO14), in which SASM precipitation was marked by the precession signal, indicating a stronger influence of the tropics (Cruz et al., 2005, Rodríguez-Zorro et al., 2020). The different climatic organization revealed the dominance of the southern hemisphere on the composition of vegetation prior to the mid-Pleistocene transition, which included signatures of taxa that currently grow at higher latitudes in cooler and more seasonal environments than Colônia, like *Acaena* and *Nothofagus* types (Fig. 4 and Supplementary Material Fig. 1).

Constraining the age-model of COL17c and the hypothetical drivers of change during the early Pleistocene at Colônia

As explained before, the SASM and the southern hemisphere fronts have been playing a major role in the input of precipitation and vegetation dynamics at Colônia's latitude. From the analysis of proxies in the previous section (5.1), we concluded that the seven alternating phases of grasses, SDF and EF, shore taxa, and organic matter input in the lake represent the effect of glacial-interglacial periods on sedimentation and surrounding vegetation (Figs. 6 and 7). The COL17c chronology from Simon et al. (2020), which was not orbitally tuned, lies between 1.497 ± 0.102 Myr and 1.347 ± 0.092 Myr, for the 51.71 to 45.99 mcd section (sedimentation rates ranging between 2 to.6 cm/kyr). Applying this chronology to the proxies reflects a seemly 41kyr cyclicity (Supplementary material Figs.2 and 3), which provides independent validation for our interpretation of the cycles as glacial-interglacial succession. Yet, due to its large uncertainties, it is necessary to refine this chronology and establish a more constrained time frame for the observed changes in the COL17c proxies which seem to favor a tuning with a 41 kyr pace. Similarly, a model with higher sedimentation rates such as insolation paced tuning would fit in the uncertainties envelope from Simon et al. (2020) and should be explored as well (Supplementary material Fig.2, 4 and 6).

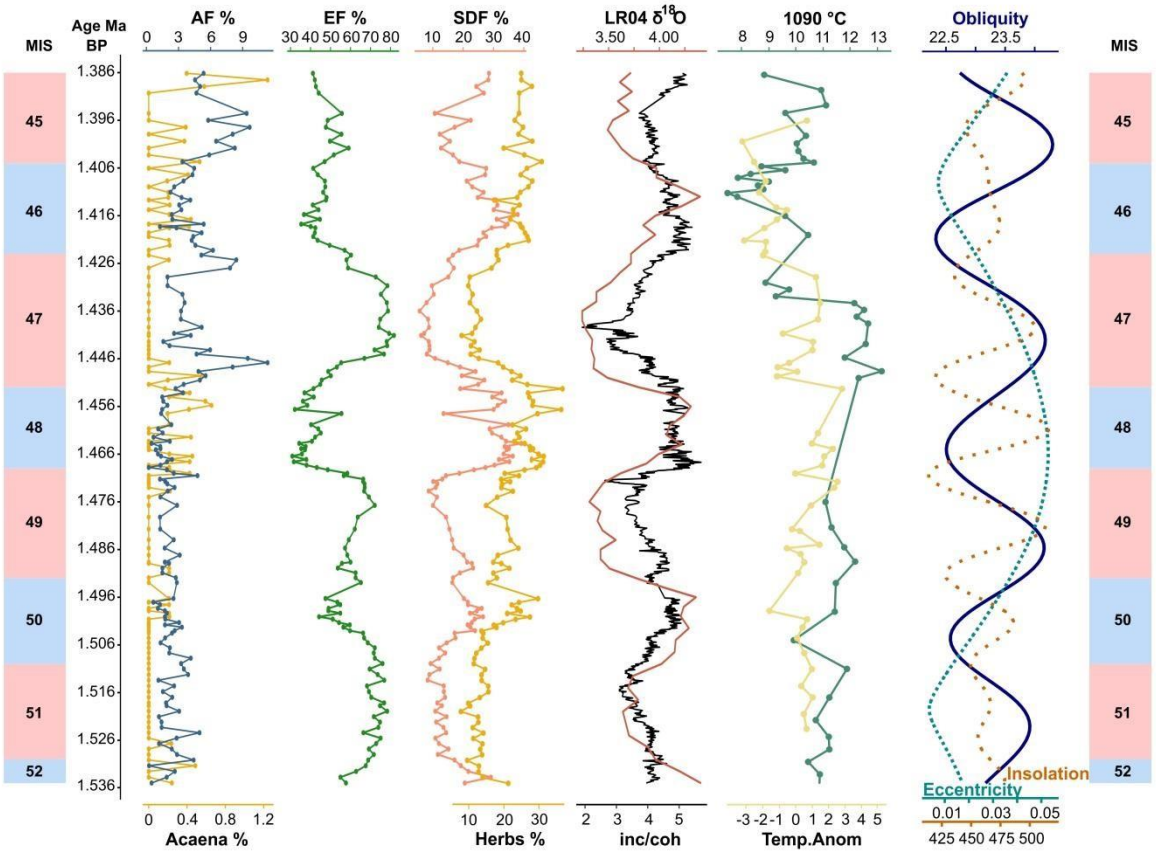

Figure 8. Early Pleistocene dynamics from the COL17c section 51.71 to 45.99 mcd. From left to right, pollen data in percentages from Araucaria, Acaena, EF, herbs and SDF. inc/coh element counts compared to the LR04 δ18O stack (Lisiecki and Raymo, 2005). In yellow, MAAT anomalies based on the soil and peat calibration protocol by Véquaud et al. (2022). In green, sea surface temperatures from the ODP-1090 record (Martínez-Garcia et al., 2010). Orbital parameters for latitude 23°52′03′′S using La2004 (Laskar et al., 2004). Blue and pink panels differentiate glacial and interglacial periods respectively, based on Lisiecki and Raymo (2005).

When using the obliquity tuning, first, we fitted the cyclicity period of XRF inc/coh to 41kyr by locally adjusting the sedimentation rate. Maximizing the correlation between XRF inc/coh and LR04 (δ18O global benthic foraminifera; Lisiecki and Raymo, 2005) resulted in five possible age models within the uncertainty ranges of the original 10Be age model. Second, we used the significant drop in temperature noticed in 47.41 and 47.19 mcd, as evidenced in MAAT and Δ°T reconstructions. We selected the ODP site 1090 SST record (Martinez-Garcia et al., 2010) to anchor this drop in temperature in time (Fig. 3 and Supplementary Material Fig. 5). This was done acknowledging the influence of the southern fronts on the current climate and during the last interglacial at Colônia as explained in the previous section and in Rodríguez-Zorro et al. (2020). Among the five possibilities, we selected the age model that best fitted the drop in temperature (at 47.41-47.19 mcd) to the observed drop in the SST record of ODP site 1090 between 1.434-1.432 Myr. The observed 5 kyr lag between both datasets was set to keep the synchronicity from the adjusted sedimentation rates and the δ18O benthic foraminifera LR04 record (Lisiecki and Raymo, 2005). This lag is within the uncertainties from both of the models. Based on these assumptions (41 kyr pace model), the obtained chronology positions the COL17c section from 1.535 to 1.386 Myr (sedimentation rates between 3 and 5 cm/kyr) (Fig. 8 and Supplementary Material Fig. 4), from MIS 52 to 45, following the glacial and interglacial cyclicity described by Lisiecki and Raymo (2005). The mean difference between this model and the original 10Be based model from Simon et al. (2020) is ca. 52.2 ± 5.6 kyr (Supplementary Material Fig. 4).With such chronology, COL17c record places better the glacialinterglacial cyclicity that was characterized in composite depth, and helps explaining

the precipitation driven cyclicity that we observe in our proxies (Fig. 8). Reduction in precipitation and longer periods of drought during glacial periods favor the expansion of grasslands and herbs, as also seen in areas that currently have a more seasonal environment in eastern Brazil (Ferreira et al., 2022). Over this region, the dry season length and therefore the changes in tree cover in orbital scales are explained by obliquity as we observe in our record. Increases in obliquity reduces the dry season length, favoring the expansion of tree cover, while there is an expansion of grasslands and reduction in tree cover if obliquity decreases (Ferreira et al., 2022). If there is an apparent SASM precipitation paced by insolation at Colônia during the early Pleistocene as it was seen during the last 95 kyr (CO14 record), we would observe that the peaks on evergreen forest will be simultaneous with high insolation phases. Using this 41kyr tuned model, we observe that three main peaks on evergreen forest are coincident with high insolation peaks at ca. 1.480, 1.456 and 1.436 Myr, indicating the plausible influence of tropical moisture brought to the region through the SASM system. Additionally, Araucaria peaks seem to be concomitant with low insolation phases after 1.45 Myr. However, we believe that most of the vegetation responses are related to the influence of southern atmospheric and ocean dynamics occurring during the studied timeframe (Martinez-Garcia et al., 2010).

Using the same approach with an insolation paced model, we adjusted the sedimentation rates to 21kyr cyclicity, which fitted better compared to a 19 or 23 kyr pace. The COL17c section is positioned between 1.393 to 1.487 Myr (sedimentation rates between 5 and 9 cm/kyr; Supplementary Material Figs.4 and 6), from MIS 49 to 46 (Lisiecki and Raymo, 2005). The mean difference between this model and the original 10Be based model from Simon et al. (2020) is ca. 39 ± 21 kyr (Supplementary Material Fig. 4). However, using a 21 kryr paced model, the expected vegetation dynamics between glacial and interglacial periods are not synchronous with global and regional dynamics and with the proposed precipitation driven cyclicity seen in the COL17c proxies in composite depth (Fig. 7 and Supplementary Material Fig.3). Only the MIS 47 (1.424 to1452 Myr) would reflect what we have identified as interglacial conditions using the composite depth description. Using this model, the insolation peaks at 1.480, 1.456, 1.436 and 1.420 Myr fit accordingly to the evergreen forest dynamics. Araucaria peaks on the contrary are not observed during glacial-interglacial transitions neither following a clear insolation pace (see CO14; Rodríguez-Zorro et al., 2020).

Considering these two age-models and based on the precipitation driven cyclicity observed in the COL17c proxies, we favor the 41kyr tuned model, which fits better to the global and regional dynamics occurring during the early Pleistocene. We believe that the lack of a clear insolation signal in our proxies applying exclusively the chronology from Simon et al. (2020) (Supplementary Material Fig.2) shows a stronger influence from the Southern ocean circulation and land sea interactions at Colônia, following a pattern of a diminished precessional force or a precessional cancellation as seen in many δ18O records (McClymont et al., 2013). Such effect has been widely reported in marine records and currently in simulation models, explained as a widespread precessional cancellation due to mixing of North Atlantic and Southern Ocean sourced deep-water masses (Morée et al., 2021). Yet, there are some continental records that have a clearer precession signals during the studied period (e.g. Lupien et al., 2022, Panagiotopoulos et al., 2020). We recognize that the insolation pace in the COL17c record might have played an additional role in the moisture input needed for EF to expand, despite the dominant influence of the southern hemisphere through the polar fronts. We are confident that our results are congruent (at least for orbital dynamics) using a model based on the 41 kyr sedimentation rates. If there are hiatuses within the studied sedimentary section, the effect would be minimal for such approach. For pollen data, we do not see drastic changes in concentration that might indicate a hiatus or loss of sedimentary record. The same pattern would account for the high resolution XRF element counts. In this sense, we acknowledge that until having a continuous and better dated record from the Colônia basin, our interpretations remain hypothetical and the changes we observe can be only interpreted as sustained changes between glacial and interglacial periods.

Based on the COL17c 41 kyr paced age-model, we observe that the continuous presence of AF since 1.535 Myr and its further increase between 1.430 and 1.386 Myr (48.40 to 45.99 mcd), together with a drop in relative temperatures, suggest a constant influence from the polar fronts up to the latitude of

Colônia. This effect can be explained by an equatorward expansion of polar air masses and a cooling of the surface ocean from the sub-Antarctic Atlantic when arctic ice sheets were not expanded (Ehlers et al., 2018; Fig. 8). This climate configuration is related to a long-term cooling trend that occurred between 1.8 and 1.2 Myr (Becquey and Gersonde, 2002; Etourneau et al., 2010; Martinez-Garcia et al., 2010; McClymont et al., 2013). During this period, the modern cold tongue emerged in the equatorial Pacific at the beginning of the Pleistocene, which developed through a direct link between the contractions in the warm pool in the Pacific along with the expansion of the polar oceans (Martinez-Garcia et al., 2010). The prolonged effect from southern air masses and the reduction of moisture during glacial periods observed at Colônia is simultaneous with sediment deposition changes driven by obliquity from 1.6 to 1.4 Myr in Antarctic Dove Basin (Reilly et al., 2021). Such record also highlights a gradual synchronization of Northern and Southern hemisphere climate after 1.4 Myr (Reilly et al., 2021). At Colônia, glacial and interglacials after 1.43 Myr (49.30 mcd) were more influenced by the polar incursions through the subtropical fronts than before, in agreement with regional SST cooling and significant glacier expansions in Patagonia after 1.5 Myr (Fig. 8) (McClymont et al., 2013; Singer et al., 2004). However, during this time frame, it is also probable that insolation frequencies might have been affecting the COL17c record, acknowledging the ice sheet re-organization and its effect in the amplitude on the southern hemisphere signal as well as the strength of obliquity and precession prior the MTP (Morée et al., 2021, Reilly et al., 2021). The obliquity signal observed in our proxies seems to be regulating the winter seasonality coming up to the latitude of Colônia synchronously with southern atmospheric and ocean circulation dynamics (Martinez-Garcia et al., 2010; Morée et al., 2021). Additionally, the differences in meridional temperature and the configuration of the polar ice sheets that characterized glacial and interglacial periods during this time frame are concomitant with our assumptions concerning variations in forest composition and OM inputs (section 5.1). Those variations were linked to a direct effect of the polar fronts and the reduced effect of inputs of tropical moisture at the latitude of Colônia, which today is linked to the ITCZ dynamics through the SASM (Cruz et al., 2005).

The scarcity of continuous continental records during the time frame of our study hampers a wider comparison of the drivers of change and the vegetation responses in the Southern Hemisphere tropics, especially to evaluate the insolation effect.

However, our record shows that Neotropical forests were very sensitive to palaeoclimatic variations before the mid-Pleistocene transition. Our unique record highlights the importance of improving continental deep drilling projects to advance our understanding of the early Quaternary climate and ecosystem dynamics. In Australia, several extinctions coincided with the earliest glaciations of the Pleistocene, highlighting the importance of having long and complete records (Jordan, 1997). At the latitude of Colônia (23°S), we show that the effects of southern climate and ocean interactions have been shaping the landscapes since the early Pleistocene. Vegetation assemblages responded to glacial-interglacial shifts, although with different intensity, demonstrating that each glaciation contained different time signatures (e.g. a precession signature for CO14 record and obliquity signature for the COL17c). Future works should include detailed characterization at millennial scale to understand the particular signatures between each glaciation. Incorporating the responses of continental settings, especially those in southern latitudes, in large scale climate fluctuations such as glacial and interglacial periods, would enable a better view of the long term climatic and environmental dynamics as a basis to assess current and future changes (Lisé-Pronovost et al., 2019), and hence, to fully understand the climate system.

Conclusions

Our multiproxy approach allowed us to reconstruct the responses of the Atlantic forest to climate changes over a period of ca.149,000 years, between 1.535 and 1.386 Myr, covering three glacials (MIS 46, 48 and 50) and four interglacials (MIS 45, 47, 49 and 51). The amount of precipitation and low temperatures of the early Pleistocene were greatly influenced by the southern latitude circulation. The vegetation growing at Colônia responded to meridional temperature differences that regulated the

input of moisture and clearly differentiate glacial and interglacial forest types. The Atlantic forest was alternately composed of EF during interglacials, and with expansion of grasses, herbs and SDF during glacials. Araucaria was observed throughout the record although with a change in amplitude when SST dropped at Colônia related to changes in the southern circulation and Antarctic early Pleistocene dynamics. The continuous presence of Araucaria at the latitude of Colônia, further north than its current distribution area, and its larger expansion after ca. 1.43 Myr revealed that mixed evergreen forests were common between 1.535 and 1.386 Myr. We show that the different responses of the early Pleistocene tropical forest were in phase with regional climate dynamics derived from marine records, such as the equatorward migration of subpolar fronts (e.g. increases on OM input, grasses and herbaceous vegetation, and SDF). The sediments from COL17c and the good pollen and proxies preservation underline the potential of this study site to test Atlantic forest responses to climate from orbital scales up to millennial variability, to characterize tropical and subtropical plant migrations, and to strengthen the Neogene and Quaternary climate-environmental dynamics from the Southern hemisphere.

Acknowledgments
Fieldwork was supported by grants from the University of Rouen, SCALE Research Federation, French Embassy at Libreville ("Service de Coopération et d'Action Culturelle"), EPHE and the French National Research Institute for Sustainable Development (IRD). This study was also supported by ANPN and IRD through LMC14 laboratory (CEA-CNRS- IRD-IRSN-MCC, France) that provided the ^{14}C analyses, Logistical support was provided by the National Agency for National Parks (ANPN, Libreville, Gabon), WCS (Libreville, Gabon) and CEDAMM (National Park, Lopé, Gabon), Research Station on Gorilla and Chimpanzee (SEGC, Gabon), and "Agence Universitaire de la Francophonie" (AUF). We also thank the institutions that made this project possible: CENAREST for research authorizations, IRET and IRAF (Libreville, Gabon), University of Science and Technology in Masuku (Franceville, Gabon), CIRMF (Franceville, Gabon) and Omar Bongo University (Libreville, Gabon). We are grateful to Laure Paradis for extracting satellite data and mapping the field of study and François Fourel to having prepared and measured the C&N isotopes of the leaves and surface sediments. We warmly thank Benoit Devillers for lending us the Innov-X XRF portable analyzer. We thanks also Daryl Codron for giving us unpublished data of $\delta^{13}C$ values from fresh plants. Thanks to Denis Thiéblemont and another anonymous reviewer for their very constructive reviews.

Data availability

The datasets used for this article will be submitted to the open access PANGAEA database once the process of peer review is complete.

Author contributions

Paula A. Rodríguez-Zorro: Conceptualization, Formal analysis, Investigation, Visualization, Validation, Writing-original draft. **Marie-Pierre Ledru:** Conceptualization, Funding acquisition, Writing- Review & Editing. **Charly Favier:** Formal analysis, Validation, Visualization, Writing- Review & Editing. **Edouard Bard:** Investigation,Validation,Writing- Review & Editing . **Denise C. Bicudo:** Investigation, Writing- Review & Editing. **Marta Garcia:** Formal analysis, Writing-Review & Editing. **Gisele Marquardt:** Investigation, Formal analysis, Writing- Review & Editing. **Frauke Rostek:** Investigation, Formal analysis, Validation,Writing- Review & Editing. **André O. Sawakuchi:** Investigation, Writing- Review & Editing**. Quentin Simon:** Investigation, Validation, Writing- Review & Editing. **Kazuyo Tachikawa:** Investigation, Validation, Writing- Review & Editing.

Declaration of competing interest

The authors declare that they have no known competing financial interests or personal relationships that could have appeared to influence the work reported in this paper.

Acknowledgements

This research is part of the project « TROPICOL » Foundation BNP Paribas « Climate Initiative » (2017–2020), Dimensions of biodiversity" FAPESP (BIOTA 2013/502970), NSF (DEB1343578) and NASA. P.A.R.Z and Q.S benefited from a postdoctoral grant from the Foundation BNP PARIBAS. A.O.S is supported by the National Council for Scientific and Technological Development-CNPq (grant 307179/2021-4). Sandrine Canal is acknowledged for macrocharcoal analyses. We thank Fresia Ricardi-Branco, Adriana Camejo and Jerlin Fernandez (University of Campinas) for their support in the field and for their help with the pollen reference collection. We are grateful to the French Embassy in Brazil for support during fieldwork in 2018. We thank the Associação ACHAVE for support at Colônia, and the Suehara family for allowing access to their property for the corings. The first author thanks Jaime Escobar (Universidad del Norte, Barranquilla) and Carlos Jaramillo (Smithsonian Tropical Research Institute) for their constant support during the writing phase of this manuscript.

References

Bard, E., Rickaby, R.E.M., 2009. Migration of the subtropical front as a modulator of glacial climate. Nature 460, 380–383. https://doi.org/10.1038/nature08189

Batalha-Filho, H., Maldonado-Coelho, M., Miyaki, C.Y., 2019. Historical climate changes and hybridization shaped the evolution of Atlantic Forest spinetails (Aves: Furnariidae). Heredity 123, 675–693. https://doi.org/10.1038/s41437-019-0234-y

Batalha-Filho, H., Miyaki, C.Y., 2016. Late Pleistocene divergence and postglacial expansion in the Brazilian Atlantic Forest: multilocus phylogeography of Rhopias gularis (Aves:
Passeriformes). J. Zoolog. Syst. Evol. Res. 54, 137–147. https://doi.org/10.1111/jzs.12118

Battarbee, R., Jones, V., Flower, R., Cameron, N., Bennion, H., Carvalho, L., Juggins, S., 2001.
Diatoms, in: Smol, J.P., Birks, H.J.B., Last, W.M. (Eds.), Tracking Environmental Change Using Lake Sediments. Volume 3: Terrestrial, Algal, and Siliceous Indicators. Kluwer Academic Publishers, London, pp. 155–203.

Becquey, S., Gersonde, R., 2002. Past hydrographic and climatic changes in the Subantarctic Zone of the South Atlantic – The Pleistocene record from ODP Site 1090. Palaeogeogr. Palaeoclimatol. Palaeoecol. 182, 221–239. https://doi.org/10.1016/S0031-0182(01)00497-7

Behling, H., 2002. South and southeast Brazilian grasslands during Late Quaternary times: a synthesis. Palaeogeogr. Palaeoclimatol. Palaeoecol. 177, 19-27

Bennett, K.D., 1996. Determination of the number of zones in a biostratigraphical sequence. New.
Phytol. 132, 155–170. https://doi.org/10.1111/j.1469-8137.1996.tb04521.x

Bennett, K., 2009. Psimpoll 4.27: C program for plotting pollen diagrams and analyzing pollen data.
Department of Archaeology and Palaeoecology, Queen's University of Belfast, Belfast, UK.

Bicudo, D.C., Tremarin, P.I., Almeida, P.D., Zorzal-Almeida, S., Wengrat, S., Faustino, S.B., Costa, L.F., Bartozek, E.C.R., Rocha, A.C.R., Bicudo, C.E.M., Morales, E.A., 2016. Ecology and distribution of Aulacoseira species (Bacillariophyta) in tropical reservoirs from Brazil. Diatom Res. 31, 199–215. https://doi.org/10.1080/0269249X.2016.1227376

Boyer,T.P., Garcia, H.E., Locarnini, R.A., Zweng, M.M., Mishonov, Alexey, V., Reagan, J.R., Weathers, K.A., Baranova, O.K., Seidov, D., Smolyar, I.V., 2018. World Ocean Atlas 2018. NOAA National centers for environmental information. https://accession.nodc.noaa.gov/NCEI-WOA18

Camejo, A.M., Ledru, M.P., Ricardi-Branco, F., Rodríguez-Zorro, P.A., Garcia, F.R., FernandezPerdomo, J. (2022). Characterization of a glacial Neotropical rainforest from its pollen and spore assemblages (Colônia, São Paulo, Brazil). Grana. 62, 81-123. https://doi.org/10.1080/00173134.2021.1976823

Carnaval, A.C., Hickerson, M.J., Haddad, C.F.B., Rodrigues, M.T., Moritz, C., 2009. Stability predicts genetic diversity in the Brazilian Atlantic forest hotspot. Science 323, 785–789. https://doi.org/10.1126/science.1166955

Clark, P.U., Archer, D., Pollard, D., Blum, J.D., Rial, J.A., Brovkin, V., Mix, A.C., Pisias, N.G., Roy, M. 2006. The middle Pleistocene transition: characteristics, mechanisms, and implications for long-term changes in atmospheric pCO2. Quat. Sci. Rev. 25, 3150-3184.

Colli-Silva, M., Pirani, J.R., Zizka, A., 2021. Disjunct plant species in South American seasonally dry tropical forests responded differently to past climatic fluctuations. Front. Biogeogr. 13. https://doi.org/10.21425/F5FBG49882

Combourieu-Nebout, N., Bertini, A., Russo-Ermolli, E., Peyron, O., Klotz, S., Montade, V., Fauquette, S., Allen, J., Fusco, F., Goring, S., Huntley, B., Joannin, S., Lebreton, V., Magri,
D., Martinetto, E., Orain, R., Sadori, L., 2015. Climate changes in the central
Mediterranean and Italian vegetation dynamics since the Pliocene. Rev. Palaeobot. Palynol.
218, 127–147. https://doi.org/10.1016/j.revpalbo.2015.03.001
Costa, L., Wetzel, C., Lange-Bertalot, Ector, H., Bicudo, D.C., 2017. Taxonomy and ecology of Eunotia species (Bacillariophyta) in southeastern Brazilian reservoirs, Bibliotheca Diatomologica.
Croudace, I.W., Rindby, A., Rothwell, R.G., 2006. ITRAX: description and evaluation of a new multi-function X-ray core scanner. Geological Society, London, Special Publications 267,
51–63. https://doi.org/10.1144/GSL.SP.2006.267.01.04
Cruz, F. W., Burns, S.J., Karmann, I., Sharp, W.D., Vuille, M., Cardoso, A.O., Ferrari, J.A., Dias,P.L.S., Viana, O., 2005. Insolation-driven changes in atmospheric circulation over the past 116,000 years in subtropical Brazil. Nature 434, 63–66.
Davtian, N., Bard, E., Ménot, G., Fagault, Y., 2018. The importance of mass accuracy in selected ion monitoring analysis of branched and isoprenoid tetraethers. Org. Geochem. 118, 58–62.
https://doi.org/10.1016/j.orggeochem.2018.01.007
de Jonge, C., Hopmans, E.C., Zell, C.I., Kim, J.-H., Schouten, S., Sinninghe Damsté, J.S., 2014. Occurrence and abundance of 6-methyl branched glycerol dialkyl glycerol tetraethers in soils: Implications for palaeoclimate reconstruction. Geochim. Cosmochim. Acta. 141, 97– 112. https://doi.org/10.1016/j.gca.2014.06.013
de Sousa, V.A., Reeves, P.A., Reilley, A., de Aguiar, A.V., Stefenon, V.M., Richards, C.M., 2020. Genetic diversity and biogeographic determinants of population structure in Araucaria angustifolia (Bert.) O. Ktze. Conserv. Genet. 21, 217–229. https://doi.org/10.1007/s10592019-01242-9
D'Horta, F.M., Cabanne, G.S., Meyer, D., Miyaki, C.Y., 2011. The genetic effects of late
Quaternary climatic changes over a tropical latitudinal gradient: diversification of an Atlantic Forest passerine: diversification across Atlantic forest. Mol. Ecol. 20, 1923–1935.
https://doi.org/10.1111/j.1365-294X.2011.05063.x
Ehlers, J., Gibbard, P.L., Hughes, P.D., 2018. Quaternary glaciations and chronology. In: Menzies, J., van der Meer, J.J.M. (Eds.), Past Glacial Environments. 2nd ed. Amsterdam, Elsevier, pp. 77–101.
Elderfield, H., Ferretti, P., Greaves, M., Crowhurst, S., McCave, I.N., Hodell, D., Piotrowski, A.M.,
2012. Evolution of Ocean Temperature and Ice Volume Through the Mid-Pleistocene Climate Transition. Science 337, 704–709. https://doi.org/10.1126/science.1221294
Etourneau,J., Schneider,R., Blanz,T., Martinez,P.2010. Intensification of the Walker and Hadley atmospheric circulations during the Pliocene–Pleistocene climate transition. Earth Planet. Sci. Lett. 297, 103-110. doi:10.1016/j.epsl.2010.06.010
Ferreira,J.Q., Chiessi, C.M., Hirota, M., Oliveira, R.S., Prange, M., Häggi, C., Crivellari, S., Nandini-Weiss, S.D., Bertassoli Jr, D.J., Campos, M.C., Mulitza, S., Albuquerque, A.L.S., Bahr, A., Schefuss, E. 2022. Changes in obliquity drive tree cover shifts in eastern tropical South America. Quat. Sci. rev. 279, 107402. https://doi.org/10.1016/j.quascirev.2022.107402
Finsinger, W., Tinner, W., 2005. Minimum count sums for charcoal concentration estimates in pollen slides: accuracy and potential errors. Holocene 15, 293–297. https://doi.org/10.1191/0959683605hl808rr
Flora do Brasil, 2020. Rio de Janeiro Botanical garden. http://floradobrasil.jbrj.gov.br (accessed 21 November 2021)
Fontana, S.L., Bennett, K.D., 2012. Postglacial vegetation dynamics of western Tierra del Fuego.
Holocene 22, 1337-1350. https://doi.org/10.1177/0959683612444144
Garcia, M.J., De Oliveira, P.E., de Siqueira, E., Fernandes, R.S., 2004. A Holocene vegetational and climatic record from the Atlantic rainforest belt of coastal State of São Paulo, SE Brazil. Rev. Palaeobot. Palynol. 131, 181–199. https://doi.org/10.1016/j.revpalbo.2004.03.007
Garcia, R. J.F., Pirani, J.R., 2005. Análise florística, ecológica e fitogeográfica do Núcleo Curucutu, Parque Estadual da Serra do Mar (São Paulo, SP), com ênfase nos campos junto à crista da Serra do Mar. Hoehnea 32, 1–48.
Graham, R.M., De Boer, A.M., 2013. The Dynamical Subtropical Front: The Dynamical Subtropical Front. J. Geophys. Res. Oceans. 118, 5676–5685. https://doi.org/10.1002/jgrc.20408
Head, M.J., Pillans, B., Zalasiewicz, J.A., TISOQS. 2021. Formal ratification of subseries for the Pleistocene series of the Quaternary system. Episodes 44, 241-247. doi.org/10.18814/epiiugs/2020/020084

Hopmans, E.C., Schouten, S., Sinninghe Damsté, J.S., 2016. The effect of improved chromatography on GDGT-based palaeoproxies. Org. Geochem. 93, 1–6. https://doi.org/10.1016/j.orggeochem.2015.12.006
Hou, A., Bahr, A., Schmidt, S., Strebl, C., Albuquerque, A.L., Chiessi, C.M., Friedrich, O., 2020. Forcing of western tropical South Atlantic sea surface temperature across three glacialinterglacial cycles. Glob. Planet. Change. 188, 103150.
https://doi.org/10.1016/j.gloplacha.2020.103150
INMET. 2021. Instituto nacional de meteorologia. http://www.inmet.gov.br
Innes, H.E., Bishop, A.N., Head, I.M., Farrimond, P., 1997. Preservation and diagenesis of hopanoids in recent lacustrine sediments of priest pot, England. Org. Geochem. 26, 565-576
Jordan, G., J. 1997. Evidence of Pleistocene plant extinction and diversity from Regatta Point, western Tasmania, Australia. Bot. J. Linn. Soc. 123, 45-71.
Jeske-Pieruschka, V., Pillar, V.D., de Oliveira, M.A.T., Behling, H. 2013. New insights into vegetation, climate and fire history of southern Brazil revealed by a 40,000 year environmental record from the State Park Serra do Tabuleiro. Veget. Hist. Archaeobot. 22, 299-314. doi: 10.1007/s00334-012-0382-y
Kegler, A., Diesel, S., Wasum, R.A., Herrero, L., Del Río, S., Penas, A. 2010. Contribution to the phytosociological survey of the primary forests in the NE of Rio Grande do sul (Brazil). Plant Biosyst. 144, 53-84. doi: 10.1080/11263500903351276
Kociolek, J., Theriot, E., Williams, D., Julius, M., Stoermer, E., Kingston, J., 2015. Centric and Araphid Diatoms, in: Wehr, J., Sheath, R., Kociolek, J. (Eds.), Freshwater Algae of North America. Ecology and Classification. pp. 653–708.
Kulikovskiy, M., Lange-Bertalot, H., Kuznetsova, I., 2015. Lake Baikal: Hotspot of endemic diatoms II, Iconographia Diatomologica 26.
Laskar, J., Robutel, P., Joutel,F., Gastineau, M., Correia, A.C.M., Levrard, B. 2004. A long-term numerical solution for the insolation quantities of the earth. Astronomy& Astrophysics 428, 261-285. 10.1051/0004-6361:20041335
Ledru, M.-P., Salatino, M.L.F., Ceccantini, G., Salatino, A., Pinheiro, F., Pintaud, J.-C., 2007. Regional assessment of the impact of climatic change on the distribution of a tropical conifer in the lowlands of South America: Tropical conifer and climatic change. Divers. Distrib. 13, 761–771. https://doi.org/10.1111/j.1472-4642.2007.00389.x
Ledru, M.-P., Stevenson, J., 2012. The rise and fall of the genus Araucaria: A Southern Hemisphere climatic connection, in: Haberle, S.G., David, B. (Eds.), Peopled Landscapes:
Archaeological and Biogeographic Approaches to Landscapes. ANU Press. https://doi.org/10.22459/TA34.01.2012.11
Ledru, M.-P., Montade, V., Blanchard, G., Hély, C., 2016. Long-term spatial changes in the distribution of the Brazilian Atlantic forest. Biotropica 48, 159–169. https://doi.org/10.1111/btp.12266
Lisé-Pronovost, A., Fletcher, M.S., Mallet, T., Mariani, M., Lewis, R., Gadd, P.S., Herries, A.I.R., Blaauw, M., Heijnis, H., Hodgson, D.A., Pedro, J.B. 2019. Scientific drilling of sediments at Darwin Crater, Tasmania. Sci. Drill. 25, 1-14. doi.org/10.5194/sd-25-1-2019
Lisiecki, L.E., Raymo, M.E., 2005. A Pliocene-Pleistocene stack of 57 globally distributed benthic δ 18 O records. Paleoceanography 20, 1–17. https://doi.org/10.1029/2004PA001071
Lorente, F., Buso, A., De Oliveira, P.E., Pessenda, L.C., 2017. Palynological Atlas 14C LaboratoryCENA/USP. São Paulo.
Lorscheitter, M.L., Ashraf, A., Bueno, R., Mosbrugger, V., 1998. Pteridophyte spores of Rio Grande do Sul flora, Brazil. Part I. . Palaeontographica Abt.B. 246, 1–113.
Lorscheitter, M.L., Ashraf, A., Windisch, P., Mosbrugger, V., 1999. Pteridophyte spores of Rio Grande do Sul flora, Brazil. Part II. Palaeontographica Abt.B. 251, 71–235.
Lupien, R.L., Russel, J.M., Pearson, E.J., Castañeda, I.S., Astrat, A., Foerster, V., Lamb, H.F., Roberts, H.M., Schäbitz, F., Trauth, M.H., Beck, C.C., Feibel, C.S., Cohen, A.S. 2022. Orbital controls on eastern African hydroclimate in the Pleistocene. Sci. Rep. 12, 3170. https://doi.org/10.1038/s41598-022-06826-z
Marchant, R., Almeida, L., Behling, H., Berrio, J.C., Bush, M., Cleef, A., Duivenvoorden, J.,
Kappelle, M., De Oliveira, P., Oliveira-Filho, A.T., Lozano-Garćia, S., Hooghiemstra, H.,
Ledru, M.-P., Ludlow-Wiechers, B., Markgraf, V., Mancini, V., Paez, M., Prieto, A., Rangel, O., Salgado-Labouriau, M.L., 2002. Distribution and ecology of parent taxa of pollen lodged within the Latin American Pollen Database. Rev. Palaeobot. Palynol. 121, 1– 75. https://doi.org/10.1016/S0034-6667(02)00082-9

Martinez-Garcia, A., Rosell-Mele, A., McClymont, E.L., Gersonde, R., Haug, G.H., 2010. Subpolar Link to the Emergence of the Modern Equatorial Pacific Cold Tongue. Science 328, 1550– 1553. https://doi.org/10.1126/science.1184480

Martínez-Sosa, P., Tierney J., Stefanescu, I.C., Dearing Crampton-Flood, E., Shuman, B.N., Routson, C. (2021). A global Bayesian temperature calibration for lacustrine brGDGTs. Geochimica et Cosmochimica Acta 305 (2021) 87–105

Matthias, I., Semmler, M.S.S., Giesecke, T., 2015. Pollen diversity captures landscape structure and diversity. J. Ecol. 103, 880–890. https://doi.org/10.1111/1365-2745.12404.

McClymont, E.L., Sosdia, S.M., Rosell-Melé, A., Rosenthal, Y. 2013. Pleistocene sea-surface temperature evolution: Early cooling, delayed glacial intensification, and implications for the mid-Pleistocene climate transition. Earth-Sci. Rev. 123, 173-193. doi.org/10.1016/j.earscirev.2013.04.006

Metzeltin, D., Lange-Bertalot, H., 1998. Tropische Diatomeen in Südamerika, 1: 700 überwiegend wenig bekannte oder neue Taxa repräsentativ als Elemente der neotropischen Flora. In Lange-Bertalot, H. (Ed.). Iconographia Diatomologica. Annotated diatom micrographs 5.

Diversity-taxonomy-geobotany. Koeltz scientific books. Königstein, Germany. pp. 695

Metzeltin, D., Lange-Bertalot, H., 2007. Tropical diatoms of South America, II : special remarks on biogeographic disjunction, Iconographia Diatomologica 18, 1-877.

Meyers, S., 2014. Astrochron: An R package for astrochronology. http://cran.rproject.org/package=astrochron

Montade, V., Ledru, M.-P., Giesecke, T., Flantua, S.G., Behling, H., Peyron, O., 2019. A new modern pollen dataset describing the Brazilian Atlantic Forest. Holocene 29, 1253–1262.
https://doi.org/10.1177/0959683619846981

Morée, A.L., Sun, T., Bretones, A., Straume, E.O., Nisancioglu, K., Gebbie, G.2021. Cancellation of the precessional cycle in δ18O records during the early Pleistocene. Geophys. Res. Lett.
48, e2020GL090035. https://doi.org/10.1029/2020GL090035

Naafs, B.D.A., Gallego-Sala, A.V., Inglis, G.N., Pancost, R.D., 2017a. Refining the global branched glycerol dialkyl glycerol tetraether (brGDGT) soil temperature calibration. Org. Geochem.
106, 48–56. https://doi.org/10.1016/j.orggeochem.2017.01.009

Naafs, B.D.A., Inglis, G.N., Zheng, Y., Amesbury, M.J., Biester, H., Bindler, R., Blewett, J., Burrows, M.A., del Castillo Torres, D., Chambers, F.M., Cohen, A.D., Evershed, R.P.,
Feakins, S.J., Gałka, M., Gallego-Sala, A., Gandois, L., Gray, D.M., Hatcher, P.G., Honorio
Coronado, E.N., Hughes, P.D.M., Huguet, A., Könönen, M., Laggoun-Défarge, F.,
Lähteenoja, O., Lamentowicz, M., Marchant, R., McClymont, E., Pontevedra-Pombal, X.,
Ponton, C., Pourmand, A., Rizzuti, A.M., Rochefort, L., Schellekens, J., De Vleeschouwer, F., Pancost, R.D., 2017b. Introducing global peat-specific temperature and pH calibrations based on brGDGT bacterial lipids. Geochim. Cosmochim. Acta 208, 285–301. https://doi.org/10.1016/j.gca.2017.01.038

Neves, D.M., Dexter, K.G., Pennington, R.T., Valente, A.S.M., Bueno, M.L., Eisenlohr, P.V., Fontes, M.A.L., Miranda, P.L.S., Moreira, S.N., Rezende, V.L., Saiter, F.Z., Oliveira-Filho, A.T., 2017. Dissecting a biodiversity hotspot: The importance of environmentally marginal habitats in the Atlantic forest domain of South America. Divers. Distrib 23, 898–909. https://doi.org/10.1111/ddi.12581

Oksanen, J., Blanchet, F.G., Kindt, R., Legendre, P., Minchin, P.R., O'Hara, R.B., Simpson, G.L., Solymos, P., Stevens, M.H.H., Wagner, H., 2015. Vegan: Community Ecology Package. R package version 2.3-0. http://CRAN.R-project.org/package=vegan.

Oliveira-Filho, A.T., Fontes, M.A.L., 2000. Patterns of floristic differentiation among Atlantic forests in southeastern Brazil and the influence of climate. Biotrop 32, 793.
https://doi.org/10.1646/0006-3606(2000)032[0793:POFDAA]2.0.CO;2

Oliveira-Filho, A.T., Budke, J.C., Jarenkow, J.A., Eisenlohr, P.V., Neves, D.R.M., 2015. Delving into the variations in tree species composition and richness across South American subtropical Atlantic and Pampean forests. Plant. Ecol. 8, 242-269. doi:10.1093/jpe/rtt058

Panagiotopoulos, K., Holvoeth, J., Kouli, K.,Marinova, E., Francke, A., Cvetkoska, A., Jovanovska,
E., Lacey, J.H., Lyons, E.T., Buckel, C., Bertini, A., Donders, T., Just, J., Leicher, N.,
Leng, M.J., Melles, M., Pancost, R.D., Sadori, L., Tauber, P., Vogel, H., Wagner, B., Wilke, T. 2020. Insights into the evolution of the young Lake Ohrid ecosystem and vegetation succession from a southern European refugium during the early Pleistocene. Quat. Sci. Rev. 227, 106044. https://doi.org/10.1016/j.quatscirev.2019.106044

Pappas, J.L., Stoermer, E.F., 1996. Quantitative method for determining a representative algal sample count. J. Phycol. 32, 693–696. https://doi.org/10.1111/j.0022-3646.1996.00693.x
Pennington, T., Prado, D.E., Pendry, C.A., 2000. Neotropical seasonally dry forests and Quaternary vegetation changes. J. Biogeogr. 27, 261–273. https://doi.org/10.1046/j.13652699.2000.00397.x
Prado, R.L., Espin Fenoll, I.C., Ullah, I., Miura, G.C.M., Crósta, A.P., Zanon dos Santos, R.P., Reimold, W.U., Elis, V.R., Imbernon, E., Riccomini, C., Diogo, L.A., 2019. Geophysical investigation of the Colônia structure, Brazil. Meteorit. Planet. Sci. 54, 2357–2372. https://doi.org/10.1111/maps.13292
R Development Core Team, 2020. R: A Language and Environment for Statistical Computing. R Foundation for Statistical Computing, Vienna, Austria.
Ravelo, A.C., Andreasen, D.H., Lyle, M., Olivarez Lyle, A., Wara, M.W., 2004. Regional climate shifts caused by gradual global cooling in the Pliocene epoch. Nature 429, 263–267. https://doi.org/10.1038/nature02567
Reilly, B.T., Tauxe, L., Brachfeld, S., Raymo, M., Bailey, I., Hemming, S., Weber, M.E., Williams, T., Garcia, M., Guitard, M., Martos, Y.M., Pérez, L.F., Zheng, X., Armbrecht, L., Cardillo,
F.G., Du, Z., Fauth, G., Glueder, A., Gutjahr, M., Hernández-Almeida, I., Hoem, F.S.,
Hwang, J.H., Iizuka, M., Kato, Y., Kenlee,B., O'Connell, S., Peck, V., Ronge, T.A., Seki, O., Tripathi, S., Warnock, J. 2021. New magnetostratigraphic insights from iceberg alley on the rhythms of Antarctic climate during the Plio-Pleistocene. Paleoceanogr. Paleoclimatol.
36, e2020PA003994. https://doi.org/10.1029/2020PA003994
Riccomini, C., Crósta, A.P., Prado, R.L., Ledru, M.-P., Turcq, B.J., Sant'Anna, L.G., Ferrari, J.A.,
Reimold, W.U., 2011. The Colônia structure, São Paulo, Brazil. Meteorit. Planet. Sci. 46,
1630–1639. https://doi.org/10.1111/j.1945-5100.2011.01252.x
Rodríguez-Zorro, P.A., Costa, M.L., Behling,H. 2017. Mid-Holocene vegetation dynamics with an early expansion of Mauritia flexuosa palm trees inferred from the Serra do Tepequém in the savannas of Roraima State in Amazonia, northwestern Brazil. Veget. Hist. Archaeobot. 26, 455-468. DOI 10.1007/s00334-017-0605-3
Rodríguez-Zorro, P.A., Ledru, M.-P., Bard, E., Aquino-Alfonso, O., Camejo, A., Daniau, A.-L., Favier, C., Garcia, M., Mineli, T.D., Rostek, F., Ricardi-Branco, F., Sawakuchi, A.O., Simon, Q., Tachikawa, K., Thouveny, N., 2020. Shut down of the South American summer monsoon during the penultimate glacial. Sci Rep 10, 6275. https://doi.org/10.1038/s41598020-62888-x
Rumrich, U., Lange-Bertalot, H., Rumrich, M., 2000. Diatomeen der Anden: von Venezuela bis Patagonien/ Feuerland. In Lange-Bertalot, H., (Ed.) Iconographia Diatomologica 9, 673.
Russell, J.M., Hopmans, E.C., Loomis, S.E., Liang, J., Sinninghe Damsté, J.S., 2018. Distributions of 5- and 6-methyl branched glycerol dialkyl glycerol tetraethers (brGDGTs) in East African lake sediment: Effects of temperature, pH, and new lacustrine paleotemperature calibrations. Org. Geochem. 117, 56–69. https://doi.org/10.1016/j.orggeochem.2017.12.003
Schackleton, N., Opdyke, N. 1977. Oxygen isotope and palaeomagnetic evidence for early Northern Hemisphere glaciation. Nature 270, 216-219. doi.org/10.1038/270216a0.
Scheer, M.B., Mocochinski, A.Y., 2009. Floristic composition of four tropical upper montane rain forest in Southern Brazil. Biota. Neotrop. 9, 51-69.
Schlitzer, R., 2021. Ocean data view, https://odv.awi.de
Seo, I., Lee, I.L., Kim,W., Yoo,C.M., Hyeong,K.,2015. Movement of the Intertropical Convergence Zone during the mid-pleistocene transition and the response of atmospheric and surface ocean circulations in the central equatorial Pacific. Geochem. Geophys. Geosyst., 16, 3973– 3981, doi:10.1002/2015GC006077
Simon, Q., Ledru, M.-P., Sawakuchi, A.O., Favier, C., Mineli, T.D., Grohmann, C.H., Guedes, M., Bard, E., Thouveny, N., Garcia, M., Tachikawa, K., Rodríguez-Zorro, P.A., 2020.
Chronostratigraphy of a 1.5±0.1 Ma composite sedimentary record from Colônia basin (SE Brazil): Bayesian modeling based on paleomagnetic, authigenic 10Be/9Be, radiocarbon and luminescence dating. Quat. Geochronol. 58, 101081. https://doi.org/10.1016/j.quageo.2020.101081
Singer, B., Brown, L.L., Rabassa, J., Guillou, H. 2004. 40Ar/39Ar ages of late Pliocene and early pleistocene geomagnetic and glacial events in southern Argentina. In Chanell, J.E.T (Ed.), Timescales of the paleomagnetic field, Geophys. Monogr.Ser. 145, 175–190.
Sniderman, J.M., Pillans, B., O'Sullivan, P.B., Kershaw, A.P., 2007. Climate and vegetation in southeastern Australia respond to Southern Hemisphere insolation forcing in the late Pliocene–early Pleistocene. Geol. 35, 41-44. https://doi.org/10.1130/G23247A.1

Sniderman, J.M.K., Porch, N., Kershaw, A.P., 2009. Quantitative reconstruction of Early Pleistocene climate in southeastern Australia and implications for atmospheric circulation.
Quat. Sci. Rev. 28, 3185–3196. https://doi.org/10.1016/j.quascirev.2009.08.006
Stockmarr, J., 1971. Tablets with spores used in absolute pollenanalysis. Pollen et Spores 13: 615– 621.
Tagliari, M. M., Vieiledent, G., Alves, J., Silveira, T.C.L., Peroni, N. 2021. Relict populations of Araucaria angustifólia will be isolated, poorly protected, and unconnected under climate and land-use change in Brazil. Biodivers.Conserv. 30, 3665-3684. https://doi.org/10.1007/s10531-021-02270-z
Taylor, J., Harding, W., Archibald, G., 2007. An illustrated guide to some common diatom species from South Africa (No. TT 282/07), Report (South Africa. Water Research Commission). Water Research Commission.
Thomé, M.T.C., Zamudio, K.R., Giovanelli, J.G.R., Haddad, C.F.B., Baldissera jr, F.A.,
Alexandrino, J. 2010. Phylogeography of endemic toads and post-Pliocene persistenceof the Brazilian Atlantic forest. Mol. Phylogenet. Evol. 55, 1018-1031. doi:10.1016/j.ympev.2010.02.003
Thomson, D.J., 1982. Spectrum estimation and harmonic analysis. Proc. IEEE 70, 1055–1096. https://doi.org/10.1109/PROC.1982.12433
Torres, V., Hooghiemstra, H., Lourens, L., Tzedakis, P.C., 2013. Astronomical tuning of long pollen records reveals the dynamic history of montane biomes and lake levels in the tropical high Andes during the Quaternary. Quat. Sci. Rev. 63, 59–72. https://doi.org/10.1016/j.quascirev.2012.11.004
Véquaud, P., Thibault, A., Derenne, S., Anquetil, C., Collin, S., Contreras, S., Nottingham A.T.,
Sabatier, P., Werne , J.P., Huguet, A. 2022. FROG: A global machine-learning temperature